Journal of Hydrology X 21 (2023) 100160

Contents lists available at ScienceDirect

Journal of Hydrology X

journal homepage: www.sciencedirect.com/journal/journal-of-hydrology-x

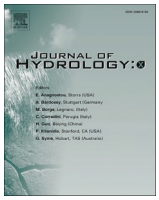

Research papers

Sensitivity of fish habitat suitability to multi-resolution hydraulic modeling and field-based description of meso-scale river habitats

David Farò [a,*], Katharina Baumgartner [b], Paolo Vezza [c], Guido Zolezzi [a]

[a] University of Trento, Department of Civil, Environmental and Mechanical Engineering, Via Mesiano 77, 38123 Trento, Italy
[b] Unit of Hydraulic Engineering, Faculty of Engineering Science, University of Innsbruck, Technikerstraße 13, 6020 Innsbruck, Austria
[c] Department of Environmental, Land and Infrastructure Engineering, Politecnico di Torino, Corso Duca degli Abruzzi 24, 10129 Torino, Italy

ARTICLE INFO

Keywords:
Ecohydraulics
River morphology
Hydro-morphological unit
MesoHABSIM
Mesohabitat

ABSTRACT

In-stream habitat models at the meso-scale are increasingly used to quantify the effects of hydro-morphological pressures in rivers. The spatial distributions of water depth and velocity represent key attributes of physical habitat. Choosing between field surveys, hydraulic modeling or their integration is made depending on available tools, technical skills, budget and time. However, the sensitivity to such choices of estimated habitat conditions suitable for biological organisms, such as fish, is poorly known.

In this study, three commonly used approaches in hydraulic-habitat modeling were compared and tested on a mountain stream, the Mareta River (NE Italy). Two approaches were based on 2D hydraulic modeling, calculated on computational meshes with varying resolution and quality: (1) high-resolution meshes derived from topographical data obtained from Airborne Bathymetric LiDAR; (2) a mesh extrapolated from topographical cross-sectional profiles. The third approach (3) was based on in-stream surveys. From these, suitable channel-area for two fish species, the marble trout (juvenile and adult), and the European bullhead (adult), were estimated.

Results showed that decreasing mesh resolution and quality affects the simulated water depth and velocity distributions, both in terms of their average and their standard deviation. The largest differences were found for the in-stream survey-based results. Morphologically complex unit types, such as steps, rapids and pools were more sensitive than simpler mesohabitats, such as glides and riffles. The most sensitive hydro-morphological unit types to the chosen approach were backwaters, glides being the least sensitive, also in terms of their suitability as mesohabitats. Despite that, a key finding is that errors are minimized when deriving habitat - streamflow rating curves at the reach scale, for which all approaches were largely able to reproduce the main characteristics of the curve, i.e. maxima, minima and inflection points.

1. Introduction

In-stream habitat models are widely used to support river restoration (Bovee, 1982; Tharme, 2003; Parasiewicz et al., 2013; Schwartz, 2016) and the definition of environmental flows (Acreman and Dunbar, 2004; Dunbar et al., 2012; Parasiewicz, 2007). They work by describing the physical characteristics of a channel, typically its hydraulic characteristics, sediment conditions and the presence and distribution of relevant features (such as covers of biophysical origins like boulders, woody debris, vegetation, etc.). Using a statistical model linking these attributes to preferences or usabilities for a given species and life-stage (Bovee, 1982; Parasiewicz, 2007; Wegscheider et al., 2021), spatial distributions of aquatic species and biological responses to hydro-morphological characteristics can then be estimated, under the assumption that habitat quality can serve as a proxy of population status and ecological integrity (Tharme, 2003; Lancaster and Downes, 2010). Due to their ability to relate hydro-morphological and ecological processes, and their relative ease of application, their use has greatly increased in the past decades (Tharme, 2003; Acreman and Dunbar, 2004). Despite habitat suitability representing a necessary but not sufficient conditions for species presence and community integrity (Anderson et al., 2006; Lancaster and Downes, 2010), the use of habitat modeling in river management has been shown to be a valuable proxy for the system ecological conditions (Lamouroux et al., 2010), allowing to define indicators that clearly correlate ecological and hydro-morphological conditions (Parasiewicz, 2007; Parasiewicz et al., 2013;

* Corresponding author.
E-mail address: david.faro@unitn.it (D. Farò).

https://doi.org/10.1016/j.hydroa.2023.100160
Received 12 July 2022; Received in revised form 1 August 2023; Accepted 7 August 2023
Available online 28 August 2023

Vezza et al., 2015).

Traditional habitat models, such as the widely used PHABSIM (Bovee, 1982), characterize in-stream habitat suitability at the "micro-scale", which refers to small (1 m^2 or smaller) river elements. This can be either done by longitudinal interpolation of suitability assessments of spaced cross-sections (Bovee, 1982; Jowett, 2010), or by defininining two-dimensional suitabilities for the reach (Steffler, 2002; Noack et al., 2013). More recently, the use of meso-scale models, that rely on a characterization of the river channel in meso-scale habitats or Hydro-Morphological Units (HMUs), such as pools, riffles and glides (Dunbar et al., 2012; Wegscheider et al., 2021), has become more common. Examples of mesohabitat modeling frameworks are MesoCASiMiR (Eisner et al., 2005), MEM (Hauer et al., 2009; Hauer et al., 2011) and the Mesohabitat Simulation Model (MesoHABSIM; Parasiewicz, 2007; Vezza et al., 2014).

One of the key outputs of habitat modeling is the habitat-streamflow rating curve for given target species and life stages, that relates the amount of suitable habitat (expressed in m^2, or as a % of the wetted channel area), and the corresponding discharge. These relationships can be used to support the definition of environmental flows, or more generally to support river rehabilitation efforts. A wide range of approaches have evolved for this purpose (Acreman and Dunbar, 2004). These comprise steady-state considerations of minimum flows, which are defined to optimize the availability of suitable habitat conditions during a specific season, or throughout the year (Jowett and Biggs, 2010; Holzapfel et al., 2014). More complex analysis involve studying the entire flow regime using time-series analysis. This is either done through simple approaches considering habitat duration curves (Bovee, 1982; Maddock, 1999), or through more in-depth analysis of flow management scenarios (Capra et al., 1995; Parasiewicz, 2007; Vezza et al., 2015).

In meso-scale habitat modeling frameworks, the physical characterization of mesohabitats is often done using in-stream field surveys to map the mosaic of Hydro-Morphological-Units (HMUs) and the distribution of habitat descriptors, such as water depth and velocity, within them. In the MesoHABSIM methodology (Parasiewicz, 2007; Vezza et al., 2014), hydraulic surveys are conducted by wading the chosen river sub-reach with a flowmeter and a meter-scale pole to measure flow velocity and depth respectively, and by surveying representative points for each HMU. However, particularly for large gravel-bed rivers and at higher flows, in-stream surveys become challenging with reduced wadeability. Hydraulic numerical models based on the solution of the shallow water Saint–Venant differential system (Vreugdenhil, 1994) are now of common use in river engineering and restoration projects (e.g. Kondolf et al., 2000; Legleiter and Goodchild, 2005; Pasternack, 2011; Parasiewicz et al., 2012; Tonina, 2013; Schwartz, 2016; Wegscheider et al., 2021). Their use can compensate wadeability issues in habitat modeling, allowing a fast and accurate reconstruction of the flow field at different discharges in streams where the shallow water assumption applies, such as piedmont and lowland rivers.

Two-dimensional (2D) numerical hydraulic models can describe complex flow patterns associated with the spatial variability of water depth, flow velocity and bed shear stress at different discharge conditions (Nelson and Bennett, 2003; Nelson, 1989), and they are increasingly used for ecohydraulic studies (Tonina, 2013). A prerequisite for accurate hydraulic modeling is the accurate representation of the topographical flow domain, described in the form of a Digital Terrain Model (DTM). The DTM is used within 2D hydraulic modeling by first converting it into a computational mesh, an ensemble of grid cells that defines the geometrical domain and boundaries of the simulated water flow. Highly accurate DTMs are particularly relevant in reaches characterized by large bedform- (or macro-) roughness, due to e.g. the presence of large boulders and other structures (Crowder and Diplas, 2000; Baumgartner, 2020), since minor topographical changes in the DTM have been shown to affect the simulated flow field (Hardy et al., 1999; Marks and Bates, 2000; Mandlburger et al., 2009). While grain-size roughness can be characterized by the choice of an appropriate roughness coefficient and turbulence model during model calibration (Morvan et al., 2010; Tonina, 2013), the representation of locally complex flow field structures, such as eddies and lateral flow divergence and convergence, will require an accurate description of the macro-roughness in the computational mesh (Crowder and Diplas, 2000; Tonina, 2013; Benjankar et al., 2015; Baumgartner, 2020). Adequate DTM quality and mesh resolution for each application hence need to be carefully selected depending on the morphological complexity of the reach, and the scope of the analysis (Pasternack et al., 2006; Gonzalez and Pasternack, 2015; Papaioannou et al., 2019). Airborne LiDAR bathymetry (ALB) is a remote sensing technology that well fits these requirements, allowing the construction of high resolution and precision DTMs (McKean et al., 2014; Tonina et al., 2019), and the detection of water surface which provides major advantages for the calibration of hydraulic models (Mandlburger et al., 2015; Baumgartner, 2020).

Prior applications of 2D hydraulic models to simulate river habitat suitability have focused on micro-scale habitat models. Conner and Tonina (2014) found differences of up to 20% in estimated micro-scale habitat suitabilities when comparing the results from a complete grid model against those obtained by the same model run on a grid interpolated from cross-sections. The largest differences were found along the stream banks and in areas characterized by complex water depth and velocity patterns. Similarly, when comparing applications of a 2D model against results from 1D modeling, which used cross-sections derived from the DTM, Benjankar et al. (2015) found that, while in some reaches the differences in habitat quantity were found to be similar, the mismatch in spatial distribution was strongest in complex morphologies. More recently, Papaioannou et al. (2019) analyzed the sensitivity of microscale habitat suitability estimates for two fish species (*Salmo pagonicus* and *Barbus balcanicus*) to the geometrical configuration of the hydraulic model domain, for a piedmont gravel-bed stream with large boulders. Both DTM (0.15 to 3 m) and computational mesh (0.3 to 3 m) resolutions were analyzed, finding that mesh resolution had a stronger effect on habitat suitabilities compared to DTM resolution. The authors suggested that, to accurately resolve reach-scale hydraulic patterns, both DTM and mesh resolution should be kept at values lower than 1 m, for a river reach with channel width in the range of 3 to 15 m. The use of a meter-scale spatial description of the river was also advocated by Pasternack (2011), who coined the term near-census to refer to comprehensive, spatially explicit observation of the landscape emphasizing the $\sim 1m$ scale as the basic building block for characterizing geomorphic processes and ecological functions in large rivers. A number of studies confirmed that such accuracy is needed to adequately represent ecological processes at a relevant scale in large rivers with wetted channel widths greater than 30 m (e.g. Pasternack et al., 2006; Gonzalez and Pasternack, 2015).

The application of meso-scale habitat models has been increasing over the past years. However, only few examples exists of their applications in gravel-bed rivers for conditions in which in-stream surveys become challenging, and when 2D hydraulic modeling is therefore used to simulate the flow pattern (e.g. Legleiter and Goodchild, 2005; Hauer et al., 2009; Parasiewicz et al., 2012; Farò et al., 2022). Effects of different accuracies and resolution of the DTM and of the derived mesh have been so far analyzed for micro-scale 2D hydraulic-habitat modeling (Conner and Tonina, 2014; Benjankar et al., 2015; Papaioannou et al., 2019), but not for meso-scale hydraulic-habitat models. A better understanding of meso-scale hydraulic-habitat models' sensitivities to different DTM and mesh resolution is therefore needed.

Here we compare three different approaches to describe the meso-scale hydraulic habitat in a river reach, and we test the sensitivity of related fish habitat suitabilities. The three chosen approaches represent typical modeling and survey-based choices to assess meso-scale habitat conditions in gravel-bed rivers, namely: (1) 2D hydraulic modeling based on high-resolution computational meshes extracted from high-resolution DTMs; (2) 2D hydraulic modeling based on a mesh derived

from cross-sectional topographical profiles; and (3) a standard in-stream survey performed according to the MesoHABSIM methodology (Parasiewicz, 2007; Vezza et al., 2014). Our specific research questions focus on how sensitive are: (1) the description of HMUs hydraulics; and (2) the estimated fish habitat suitabilities on the choice of approach used to quantify the hydraulics of the mesohabitats.

In particular, we wanted to test the sensitivity of the following variables to the choice of the hydraulic approach:

1. the frequency distribution of the hydraulic variables (water depth and velocity within HMUs). Furthermore we analyzed whether differences at the HMU type level could be identified;
2. fish habitat suitability estimates by HMU type;
3. the derived habitat-streamflow rating curve at the reach scale.

Four different meshes with varying resolutions and quality have been compared for 2D hydraulic modeling: three high resolution triangular computational meshes built on a regular grid of varying resolution (0.25, 0.50 and 1.00 m) based on high quality ALB-derived DTMs of the same resolution; and a low quality mesh, with a cell size of 1 x 1.5 m, which was interpolated from topographical cross-sectional profiles. The 2D hydraulic modeling results based on the most refined mesh (R25 mesh with a resolution of 0.25 m), were used as reference against which to compare all other results. While not implying that the reference (R25 mesh) provides a correct representation of the hydraulics in the reach, our choice of a reference simulation has been functional to compare how different the outcomes of each approach are at different spatial scales.

2. Materials and methods

2.1. Workflow of the study

A summary of the workflow of our analysis is represented in Fig. 1. The topo-bathymetry of the study area was acquired by ALB, from which a set of three regular grid meshes with varying resolutions and a cross-sections based computational mesh were derived (Section 2.3; in yellow in Fig. 1). Based on the derived meshes and calibration data acquired through the ALB survey, a 2D hydraulic model was set up for each mesh, and HMU hydraulics computed (sec. 2.3; in light blue in Fig. 1). The mosaic of HMUs and their hydraulics was acquired through field surveys at different flows based on the MesoHABSIM methodology (Section 2.4; in brown in Fig. 1). Presence/absence habitat suitabilities at the meso-scale were estimated by simplified mesohabitat models (Section 2.5; in green in Fig. 1). And finally, a statistical analysis was conducted to study

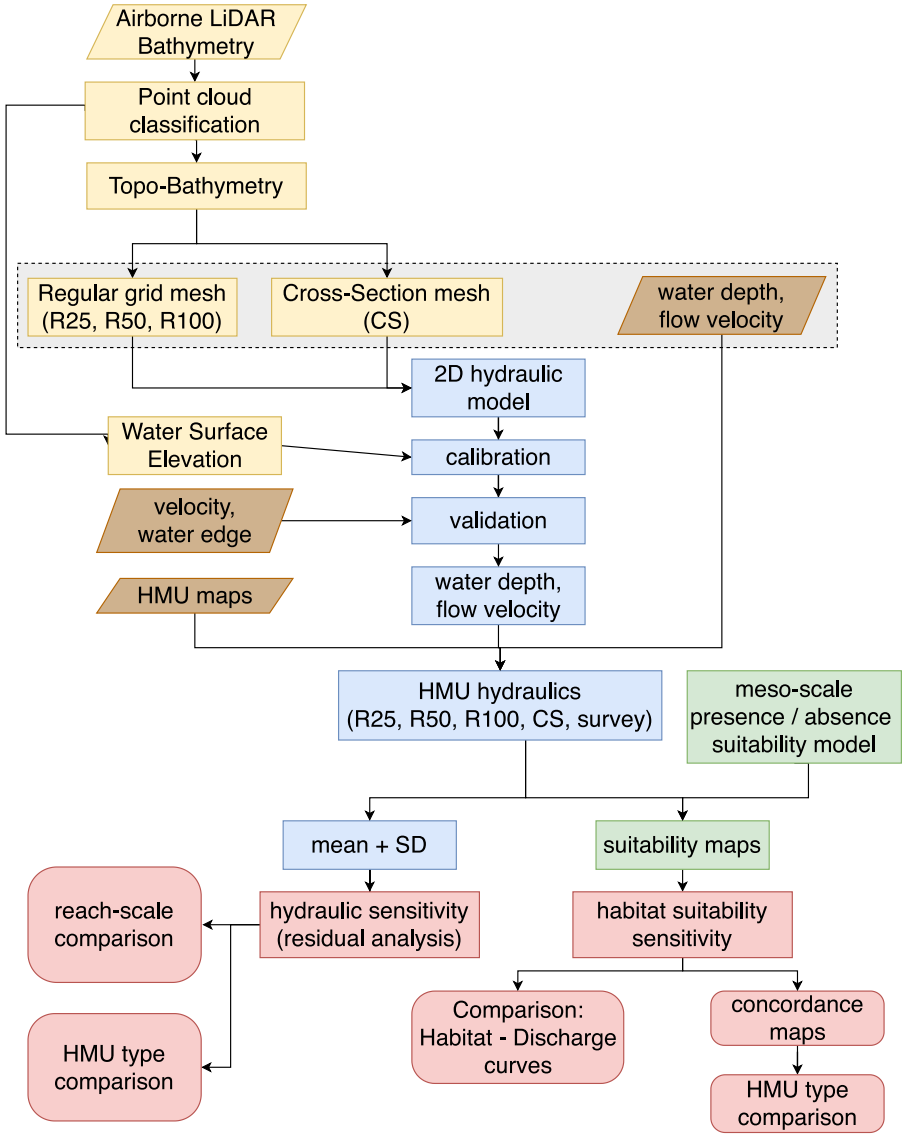

Fig. 1. Illustration of the analysis workflow. The steps of the workflow are grouped into categories: acquisition and preparation of the DTMs and meshes (yellow); description of the reach hydraulics (2D hydraulic modeling; blue); mapping of HMUs and their hydraulics, according to the MesoHABSIM methodology (brown); habitat suitability comparison (green); statistical analysis of the hydraulics and habitat suitability of the HMUs (light pink). The three approaches used to derive the hydraulic description of the reach are highlighted through a light grey box. Parallelograms represent surveyed data; rectangles denote processes; rounded shapes show final results.

the sensitivity of the probability distributions of water depth and velocities and of their derived habitat suitabilities on the hydraulic domain data sources (Section 2.6; in light pink in Fig. 1).

2.2. Study area

The study was conducted on the Mareta River (Mareiterbach in German, from this point onwards referred to as Mareta River; Fig. 2), a gravel-bed river located in the central-eastern Italian Alps, in the region of South-Tyrol. The river is characterized by a nivo-glacial flow regime and high sediment dynamics. Over the last century it has been heavily modified by channelization, construction of grade-control structures and intense phases of gravel mining, which caused changes in the active channel width and in its morphological pattern. Following works done in 2009 (Zerbe et al., 2019), in which all check-dams and bank protections have been removed, a 3 km-long reach of the river located few kilometers upstream the city of Sterzing/Vipiteno was restored to a braided morphology. The restored reach has a catchment area of 206.53 km^2 and an average slope of $\sim 1\%$. Its mean, median and mean-annual-low flows (at the hydrometric station) are respectively 7.15, 4.7 and 1.57 m^3/s, while streamflow values at 2, 10 and 100 return intervals are respectively 72.5, 125 and 183 m^3/s. Within the restored reach a 1.5 km-long section was selected as study area to run 2D hydraulic simulations, and a shorter sub-reach of approximately 350 m for the mesohabitat surveys, selected as representative of the morphological characteristics of the larger reach, sensu Belletti et al. (2017). The modeled reach is characterized by an average (wetted) channel width at the lowest flow of $1.7\,m^3/s$ of $\sim 17\,m$ (which increases to 21 and 31 m respectively at the higher surveyed discharges of 3.2 and 10.4 m^3/s, with minimum and maximum values for the surveyed discharges of 7 and 41 m). Substrate composition of the reach ranges from cobbles to large boulders, with characteristic grain-sizes (determined through line-sampling according to Fehr, 1987) of: $D_{50} = 48.9 \pm 13.7\,mm$ and $D_{84} = 88.9 \pm 27.2\,mm$ (average $\pm$ std. deviation). Macro-roughness elements, in the form of large boulders that were artificially placed in the reach in a previous river rehabilitation project, have a horizontal average dimension of $\sim 1.5\,m$ (Baumgartner, 2020).

2.3. Airborne LiDAR Bathymetry (ALB) survey and 2D hydraulic modeling

The morphology of the riverbed was acquired by a high-resolution airborne LiDAR bathymetric survey on December 15th, 2016. The ALB flight was carried out by the AirborneHydroMapping GmbH (www.ahm.co.at) company, as part of the FHARMOR project (Farò et al., 2018). The flight was conducted during the lowest surveyed flow ($1.7\,m^3/s$). As a first post-processing step the acquired points were georeferenced by manually adjusting the point cloud to fit Ground Control Points measured with a cm-grade GPS-RTK system from large visible objects. The georeferenced points were then classified into categories (water surface, river bathymetry and land). Finally, a refraction correction was applied to all bathymetrical points in accordance to Snell's law, using constant refraction coefficients (1.33 for water, and 1.00029 for air). Efforts were undertaken to preserve the complexity of the morphological structures, resulting in two classified point clouds of the topo-bathymetry (with a mean point density of 140 points/m^2), and a reconstruction of the water surface elevation (WSE). All post-processing was done using the HydroVish software (Steinbacher et al., 2021). Quality control points for the bathymetrical ALB (bathymetry and WSE) survey were collected using a total station (Leica Viva TS15) along 12 cross-sections within the channel (and additional points for WSE inbetween cross-sections). Cross-sections were selected approx. every 20 m (Fig. S1, supplementary materials), so as to represent the main morphological structures within the reach. An average of 11 points were measured at each cross-section (for a total of 146 points). A high level of agreement was found between ALB-measured topo-bathymetry and WSE and the surveyed quality check points. The difference between ALB and in-stream measured values for respectively topo-bathymetry and WSE yielded median values of -0.01 and -0.02 m, and RMSE respectively of 0.03 and 0.04 m (Baumgartner, 2020, Fig. 4.1.2).

To lower the computational effort in further applications, a reduction of the amount of data was performed by projecting the points onto a regular raster grid, with the heights of each cell computed as the mean of the surrounding points. DTMs based on the original classified data point cloud were extrapolated in the form of raster data sets with a regular grid resolution of 25 (R25), 50 (R50) and 100 cm (R100). Additionally, rasters for WSE with the same resolutions were created. This were subsequently used to calibrate the hydraulic model at the low flow discharge. The DTMs were then converted to regular triangulated meshes. All meshes were generated using the software Surface-Water Modelling System (SMS; by Aquaveo).

Due to economic constraints, it is common practice to reconstruct the bathymetry of wadable river sections from cross-section profile surveys. To compare the effect of using traditional bathymetric surveys or high-resolution ALB-based ones on habitat modeling at the meso-scale, a DTM based on cross-sections was also created from the original DTM, from which a further computational mesh (CS) with rectangular elements of 1.0 x 1.5 m was extracted. The topographic cross-sections (Fig. S2) were extracted from the high resolution raster, keeping a variable distance

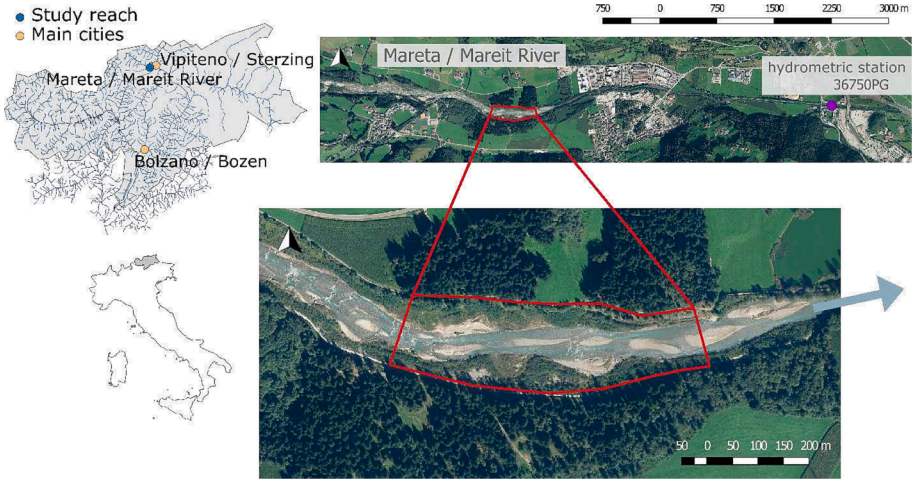

Fig. 2. Map of the study area of the Mareta River. The location of South Tyrol within Italy and of the study reach within the province are shown. The study area is highlighted in red. Downstream of the reach the hydrometric station (36750PG) provided the hydrological time series.

between the cross-sections of 4 to 42 m, a measure smaller than the average width of the active river corridor. Smaller distances were elected in topographically complex areas (which were visually assessed in the field and based on the available high-resolution DTM), where they were essential to preserve the shape of the riverbed.

Table 1 presents a comparison of the different implemented meshes, in terms of: their geometrical characteristics (number of nodes, point density and mesh geometry); computation time for a simulation run; the adimensionalized grid size in relation to wetted channel width (average, minimum and maximum) and average size of macro-roughness elements. A visual comparison between the different computational meshes (R25, R50, R100 and CS), highlighting the decrease in detail as a consequence of a decrease in point density and of interpolation between areas (CS), is depicted in Fig. 3.

Hydraulic modeling of the studied reach was performed using the hydraulic model HYDRO_AS-2D (Nujić, 2017). The simulation is based on a 2D depth-averaged shallow flow model with spatial discretization according to a finite-volume method, and implementing a second order explicit Runge Kutta time discretization scheme. The convective flow of the 2D model is based on the upwind-scheme by Pironneau (1989). A parabolic eddy viscosity model with a constant value of 0.6 for the turbulent viscosity coefficient was used. No secondary flow correction was implemented. A value of 0.01 m was set for wetting/drying computations. The simulations were run on a computer with 32 GB of ram and four cores (Intel(R) Xeon(R) CPU E3-1240 v5 @3,50 GHZ) using two HYDRO_AS-2D licenses, and average run times for each simulations recorded.

Calibration of the model was performed at the constant discharge of 1.7 m^3/s in two steps, and carried out by minimizing Root-Mean-Squared Error (RMSE) values between the simulated and ALB-surveyed water surface elevations (WSE). During the first calibration step, an optimal (i.e. minimizing the RMSE) uniform roughness coefficient (Gauckler-Strickler k_{st}) was derived for the reach, by running multiple istances of the hydraulic simulation with varying uniform roughness coefficient in the range $k_{st} = 17-30 m^{1/3}/s$. In the second calibration step, due to the highly structured and morphologically diverse river bed bathymetry, a spatially variable (SV) roughness classification was done to improve modeling results. The values obtained during the first calibration step were used as basis for this second calibration step. Resulting spatially variable Gauckler-Strickler coefficients range from $k_{st} = 15 m^{1/3}/s$ for non-fluvial artificial boulders, to $k_{st} = 34 m^{1/3}/s$ for smoother plane-bed structures (Fig. S3). Regions of distinct substrate compositions were manually defined using available orthophotos, the ALB-derived point cloud and hydraulic modeling results. The calibration of the spatially variable roughness zones was carried out using the R50 mesh. To ensure comparability between results, the resulting roughness distributions from the R50 mesh were then transferred to the remaining meshes. For the calibration, a steady discharge of $1.70 m^3/s$ was defined as upstream boundary conditions, which was measured during the ALB flight using the Sontek FlowTracker2 handheld device.

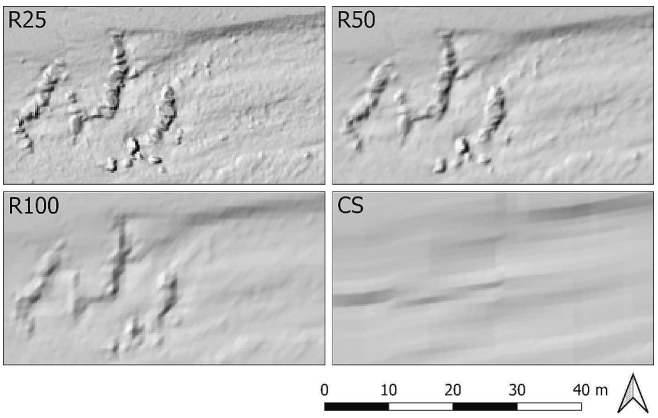

Fig. 3. Reproduction of topographical details for the Mareta River for the four analyzed meshes (R25, R50, R100 and CS).

Following standard calibration and validation procedures (Blocken and Gualtieri, 2012; Wright et al., 2017), the predictive performance of the model and the differing meshes was assessed against a data-set (Fig. S1, in supplementary materials) of surveyed flow velocities, which were measured at the calibration discharge (Q = 1.7 m^3/s) but independently of the WSEs used to calibrate the model, and water edge locations measured along the banks (at Q = 10.4 m^3/s). To assess the ability of the model to correctly represent water velocities, point-sampling over two cross-sections were collected at low flow (1.7 m^3/s). Cross-sections were selected in a wadable section of the river, and a total of 30 points were collected at regular intervals (Fig. S1). Velocities were measured at three different elevations within the water column, corresponding to fractions of 0.2, 0.4 and 0.8 of the local water depth (measured from the bottom), and then averaged to obtain depth-averaged velocity values to be compared with the outputs of the 2D, depth-averaged hydraulic simulations. Additionally, model performance at higher discharges was assessed ($Q = 10.40 m^3/s$) by comparing the position of modeled and surveyed water-edges. For the assessment, we computed planar distances between the measured water edges and the corresponding closest modeled wet points (defined as positive if the water edge was in a dry area compared to model results, and negative if it fell within the modeled wetted channel), and vertical differences (computed as the difference between the measured height and the WSE of the closest wet modeled point). To assess level of agreement, commonly used metrics (Barker et al., 2018) have been computed

Table 1
Characteristics of the computational meshes used in the 2D hydraulic modeling and computation time for a simulation run. The following characteristics are shown: DTM resolution and corresponding mesh; total number of nodes; point density (in $pts./m^2$); average computation time for a simulation run; adimensionalized grid size (in %) in relation to the wetted channel width (average, minimum and maximum), and to the average size of macro-roughness elements; and goodness-of-fit between modeled and surveyed values (RMSE and R^2) for topo-bathymetry.

DTM	Mesh	Number of nodes	Point density (Pt/m^2)	Mesh elements	Computation time (h min)	Adimensionalized grid size (in %) in relation to				Goodness of fit
						channel width			macro-roughness elements	topo-bathymetry
						avg.	min	max		RMSE (m)
regular grid (0.25 x 0.25 m)	R25	~2.141.000	~15 Pt/m^2	triangular	6 h 50 min	2	6	1	17	0.05
regular grid (0.5 x 0.5 m)	R50	~547.000	~4 Pt/m^2	triangular	50 min	3	13	2	33	0.06
regular grid (1 x 1 m)	R100	~138.000	~1 Pt/m^2	triangular	5 min	7	25	3	67	0.07
interpolated from cross-sections (1.0 x 1.5 m)	CS	~77.000	~0.5 Pt/m^2	rectangular	1.25 min	7 x 10	25 x 38	3 x 5	67–100	0.13

between modeled (x_{mod}) and measured (x_{meas}) values: average and standard deviation of bias ($x_{mod} - x_{meas}$); regression metrics in the form of slope and intercept (coefficient. ± standard error), computed for measured vs. modeled values (Piñeiro et al., 2008); coefficient of determination R^2; RMSE; Nash–Sutcliffe efficiency (NSE).

Additionally, we checked that differences in water depth between modeled and ALB-derived values were consistent across all HMU types.

Table 1 presents a comparison of the different implemented meshes, in terms of: their geometrical characteristics (number of nodes, point density and mesh geometry); computation time for a simulation run; the adimensionalized grid size in relation to wetted channel width (average, minimum and maximum) and average size of macro-roughness elements.

More details about the processing of ALB data, the construction of the DTMs, and the calibration and validation of the 2D hydraulic modeling can be found in Baumgartner (2020).

2.4. Mesohabitat field data collection and hydraulics survey

Surveys have been conducted in the years 2017 to 2018. While some morphological changes could be observed within the modeled reach, these were negligible in the sub-reach in which HMUs were surveyed (Baumgartner, 2020).

The mosaic of HMUs at varying discharges was repeatedly mapped at the study reach according to the MesoHABSIM methodology (Parasiewicz, 2007; Vezza et al., 2014). The following HMU types have been identified in the reach: backwater, rapid, riffle, step, glide and pool (see Table S1 in suppl. materials for a description of their main hydromorphological characteristics).

HMUs were mapped on the Mareta River using a portable GIS system connected to a TruPulse 360B laser rangefinder. The survey was georeferenced using the GPS system of the Getac PS336, running ESRI Arcpad 10.2.5. The HMU mosaic was recorded at three discharges, from low to mid flows, at $Q = 1.7$ (February 2017), 3.2 (April 2018) and $10.4\,m^3/s$ (June 2018). Fig. 4 shows the mapped HMU mosaics (a), the hydrology of the reach for the project years (b), and the flow duration curve (c).

Within each HMU a minimum of 7 measurements of water depth (D) and depth-averaged velocity (V) were conducted. Water velocity was measured at $0.4{\cdot}D$ from the bottom, as commonly prescribed for hydrometric and hydraulic habitat measurements. To ensure a representative coverage of the hydraulic distribution of the parameters within each HMU, surveys were conducted following a randomly-stratified approach (Parasiewicz, 2007), with an average point density of $0.044\,pts./m^2$ (with a minimum and maximum of 0.007 and $0.335\,pts./m^2$ respectively).

2.5. Meso-scale fish habitat suitability models

Habitat suitability is estimated by means of simplified habitat suitability models for the considered species and life-stages, which consider only the hydraulic parameters water depth and velocity as habitat attributes. The implemented simplified models were constructed based on literature-based information and field observations (Adamczyk et al., 2019; Negro et al., 2021). Using as a basis exisiting statistical habitat suitability models (Vezza et al., 2017; Negro et al., 2021), which had been previously validated in nearby streams with similar hydromorphological and climatic characteristics through electrofishing and snorkeling surveys (Carolli et al., 2017; Negro et al., 2022), conditional habitat suitability criteria were built by defining the threshold values of the hydraulic descriptors that maximize the HMU classification performance in terms of probability of presence/absence. In accordance with the procedure implemented in the MesoHABSIM approach (Parasiewicz, 2007; Vezza et al., 2017), water depths and flow velocities are discretized into bins with widths of respectively 15 cm and 15 cm/s. For given distributions of depth and velocity in a specified HMU, the model yields as a result the estimated presence or estimated absence of the chosen species within the HMU. Habitat suitability for the reach (absolute value of wet channel area, in m^2) is then computed as the sum of the areas of all suitable mesohabitats (HMUs), with suitability occurring

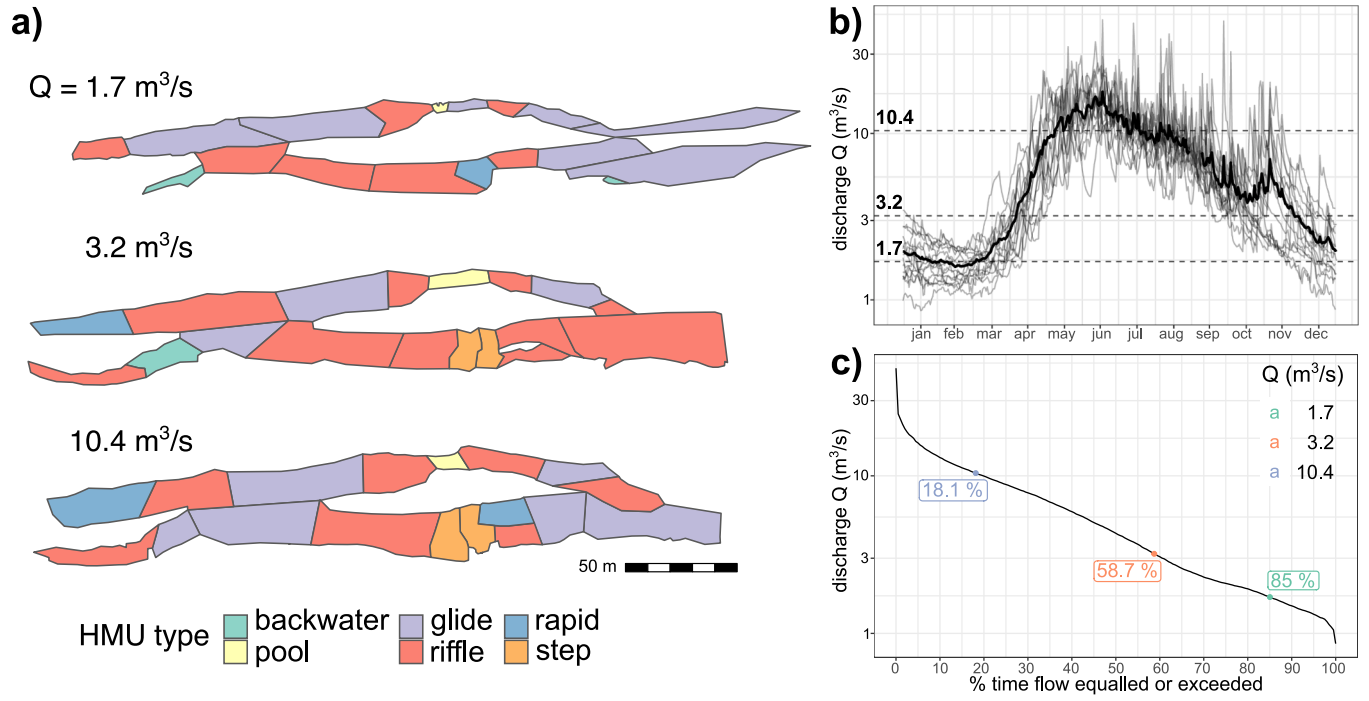

Fig. 4. Mesohabitat and hydrological characteristics of the study reach on the Mareta River (as measured by the hydrometric station 36750PG). (a) mapped HMU mosaics at increasing discharges are shown; (b) gauged hydrographs. Individual hydrographs for the years 2005 to 2019 are shown in light grey, while the average daily discharge is highlighted in black. The dotted horizontal lines visualize the discharges of the three mesohabitat surveys. In (c), the flow duration curve for the 2005–2019 period is depicted, and the surveyed discharges highlighted with the correspondent exceedance time percentage.

when the model indicates probability of presence for the considered HMU.

Models were developed for the following target species and life-stages, selected as representative for the reach (as reported by the office for "Fauna, Hunting and Fisheries", of the Autonomous Province of Bolzano): adult and juvenile marble trout (*Salmo marmoratus*); and adult European bullhead (*Cottus gobio*). The conditional models are shown in Fig. 5.

Note that in the MesoHABSIM approach, mesohabitats are evaluated using a larger variety of habitat descriptors (water depth, flow velocity, substrate composition, cover types and water surface gradient). Habitat evaluation focusing only on water depth and flow velocity was chosen for the purpose of this work, given its aim of comparing the sensitivities of estimated habitat suitabilities to hydraulic descriptions of HMUs obtained using different surveying and modeling approaches.

2.6. Sensitivity of HMU hydraulics and habitat suitability

2.6.1. Sensitivity of HMUs hydraulics

Sensitivity of water depth and velocity within each HMU to the choice of hydraulic description approach was tested by computing mean and standard deviation (SD) of the distributions. Mean and SD were then compared with the values of the reference configuration, which is represented by the 2D hydraulic modeling based on the R25 mesh. We remark here that our choice of a reference simulation allows comparing how different the outcomes of each approach are at different spatial scales and does not imply that its results provide the most accurate

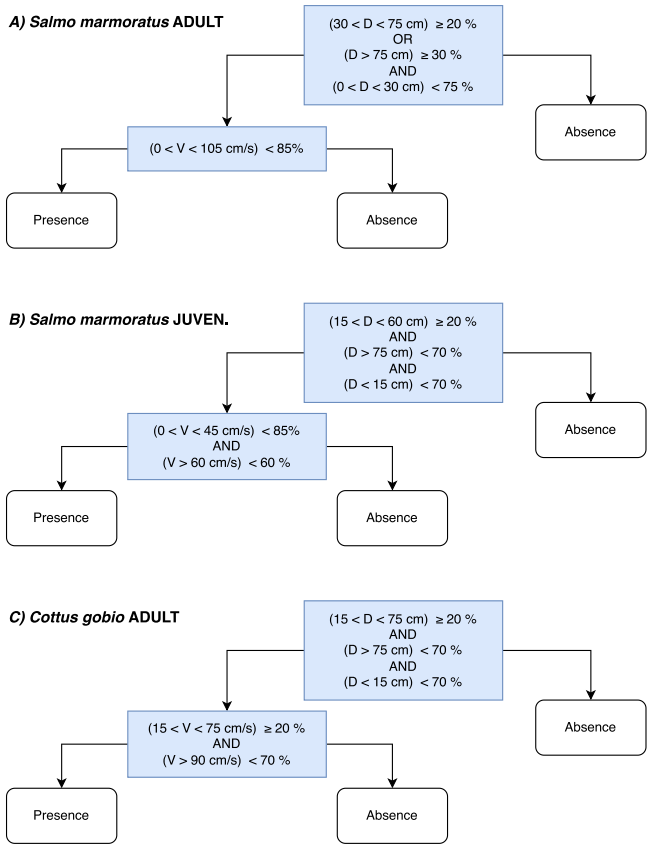

Fig. 5. Conditional biological models, for the species marble trout (*Salmo marmoratus*, juvenile and adult) and European bullhead (*Cottus gobio*, adult). These simplified models have been derived from more complete, multivariate models that account for all relevant environmental descriptors as defined within the MesoHABSIM methodology. Given the focus of this work, only the hydraulic variables (shaded in light blue) water depth (D) and velocity (V) are used here.

representation of the actual flow field. Residuals ($\overline{x}_{res}$) were then computed by normalizing each value ($\overline{x}$) against its reference ($\overline{x}_{ref}$) according to the following equation:

$$\overline{x}_{res} = \frac{\overline{x} - \overline{x}_{ref}}{\overline{x}_{ref}} \cdot 100\%$$

The mean and SD of different water depth and flow velocity distributions were compared as a sensitivity test. The comparison was performed both at the reach and at the HMU scale. For the reach-scale analysis, all HMUs have been grouped together regardless of their classification into HMU types. In the HMU-scale analysis, units are separated into HMU types, and compared with each other.

Using a Kruskal–Wallis test, the similarity of residuals across modeled discharges for all tested approaches was assessed. To increase sample size, particularly for under-represented HMU types such as pools and backwaters, and given the resulting similarity (Table S3), all residuals were pooled together, and assessed independently of discharge.

For the reach-scale analysis, slope and intercept of the linear fit between reference to comparison values, the coefficient of determination (R^2) and the Root-Mean-Squared-Error (RMSE) were computed by comparing the values of mean and SD for each approach (R50, R100, CS and survey) against those of the reference (R25). Additionally, the following descriptive statistics referring to residual differences ($\overline{x}_{res}$) were analyzed: median and its 95%-Confidence Interval (C.I. 95%); mean; SD; minimum (min) and maximum (max). A two-sided Wilcoxon signed-rank test was performed to assess whether the choice of approach significantly affected the results, positively or negatively (null hypothesis $H_0 : \mu(\overline{x}_{res}) = 0$; alternative hypothesis $H_a : \mu(\overline{x}_{res}) \neq 0$).

For the HMU-scale analysis, we assessed to which extent distributions of hydraulic parameters for different HMU types are sensitive to the choice of approach. This was assessed by comparing two sensitivity ranges, which have been defined as follows: the "median range" computed as

$$\left| max\left(median\left(x_{approach}\right)\right) - min\left(median\left(x_{approach}\right)\right) \right|$$

and the "total range"

$$|max(x) - min(x)|$$

Here the *median* $(x_{approach})$ was computed on all x residuals for a HMU type and for each approach. Larger values of the sensitivity ranges indicate a higher sensitivity towards the choice of hydraulic descriptive approach, in terms of their median and absolute values.

2.6.2. Sensitivity of mesohabitat suitabilities

A first comparison was performed at the HMU scale. Presence/absence suitabilities were estimated for each approach (R50, R100, CS and survey) and compared against the reference (R25). Suitability maps were created for the 3 analyzed discharges, from which "agreement (or concordance) maps" were derived. For each HMU habitat suitability can take the discrete values of 0 or 1, indicating respectively estimated absence or estimated presence for the species and life stage. Agreement is counted as 1 when an HMU of the comparison map has the same value as the reference map (i.e. having 1 and 1, or 0 and 0). When the values are different (i.e. 0 and 1, or 1 and 0), the value 0 is assigned (disagreement). Concordance maps express the frequency of agreement between approaches. The following metrics are computed to assess agreement to reference: the chance-corrected Cohen's Kappa (Fleiss, 1971), comparing agreement to reference for all HMUs within the reach by species and life stage, and by HMU type; percentage of "full agreement" (i.e. all cases where agreement was observed for all considered approaches) for each HMU type. The following benchmarks have been proposed by Landis and Koch (1977) for Kappa (k) values interpretation: < 0, no agreement; 0–0.20, slight agreement; 0.21–0.40, fair agreement; 0.41–0.60, moderate agreement; 0.61–0.80, substantial agreement; 0.81–1.0, almost perfect agreement.

A second comparison was based on the habitat-flow rating curves (HQ-curves), by visually comparing the shapes of the curves, and by computing the level of agreement using R^2 and the normalized RMSE (nRMSE), computed as the ratio between RMSE and the maximum value from the reference HQ-curve.

3. Results

3.1. Hydraulic model calibration and validation

A summary of calibration and validation results is presented in Table 2. Scatterplots of the comparisons can be found in the supplementary materials (Fig. S4 for the calibration results; Fig. S5, S6 and S7 for the validation results). The best results are achieved with the R25 mesh, that was best able to accurately predict modeled velocities at low flow (RMSE of 0.13 m/s and 0.83 NSE) and had the highest agreement in terms of modeled water's edges at the highest modeled flow (RMSE of 0.12 and 1.14 m respectively for WSE and planar distance). The worst performance was achieved with the CS mesh, which had an RMSE of 0.27 m/s for predicted velocities (NSE of 0.28), and the highest bias and error for predicted water edges at the highest flow (RMSE of 0.16 and 3.04 m respectively for WSE and planar distance).

Only minimal differences in water depth between modeled (R25) and ALB-derived values were observed, also when accounting for HMU type (Fig. S8).

3.2. Mesohabitat surveys

A total of 54 HMUs were mapped across the three surveyed discharges, with 18 units mapped for each surveyed discharge (1.7, 3.2 and 10.4 m^3/s). The most abundant surveyed HMU types were glides (16 or 29.6 %) and riffles (24 or 44.4 %), while the other unit types were present in lower percentages (rapids, 4 or 7.4 %; steps, 4 or 7.4 %; pools, 3 or 5.6 %; backwaters, 3 or 5.6 %). Wetted channel areas, computed based on the mapped HMUs, were of 6070.3, 7617.9 and 8355.4 m^2 respectively for the discharges 1.7, 3.2 and 10.4 m^3/s. Average water depth for the reach increased from 0.26 to 0.46 m, from the lowest (1.7) to the highest surveyed flow (10.4 m^3/s). Average flow velocity increased from 0.48 to 1 m/s (Table S2).

3.3. Sensitivity of HMUs hydraulics

Modeled water depth and velocities based on the R25 mesh are shown in Fig. 6 (see also Fig. S9 and Table S2 for a comparison of depth and velocity distributions). The figure also depicts the spatially distributed percentual differences with modeled depth and velocities for R50, R100 and CS. Differences increase with decreasing mesh resolution. While they are minimal for the R50 mesh, a consistently higher disagreement can be found for the R100 mesh, and even larger differences are observed in the case of the CS-based hydraulic modeling. The largest differences are observed close to the shore, or in highly morphologically complex areas, where e.g. flow expansion or contraction can be observed, or in and around steps and other complex morphological structures.

Differences in HMU area between the approaches were minimal. Only backwaters were always smaller in the hydraulic simulations compared to the surveyed areas, showing quite substantial differences (Fig. 6; Fig. S10).

Table 3 summarizes the level of agreement with reference values (R25 mesh) of mean and SD of the frequency distributions of depth and velocity for R50, R100, CS and survey and for each mapped HMU. The R50 and R100 results agree quite well with the R25 results ($R^2 > 0.95$ for all variables), while a higher discrepancy is found in the CS model, as confirmed by the lower values of R^2, particularly for the mean and SD of velocity. Overall, regardless of the chosen mesh, a higher agreement (higher R^2 and lower RMSE values) is found in terms of depths compared to velocities. The highest disagreement for all metrics is found with reference to the field-surveyed distributions, with a higher agreement for average velocities ($R^2 = 0.788$) than for average depths ($R^2 = 0.576$).

When comparing normalized residuals for the mean and SD of the HMU-based frequency distributions of water depth and velocity (Fig. S11), no significant differences were found for residuals grouped by discharge Q, with the exception of the water depth SD for R100 ($\chi^2_{(2)} = 7.39$), CS ($\chi^2_{(2)} = 9.64$) and survey ($\chi^2_{(2)} = 8.68$), for which a statistically significant difference (Kruskal–Wallis test, $p < 0.05$) was found (Table S3, in supplementary materials). The values corresponding to the three discharges were therefore grouped together for further analysis. It could further be observed that distribution of the residuals around zero is independent of the magnitude of the reference value. Only depth values (with a mean < 0.1 m and a SD < 0.05) are slightly affected.

The median residual difference of the HMU mean water depth increased with decreasing mesh resolution and quality, with median values (in %) of −1.9, −3.5 and −7.6 respectively for the R50, R100 and CS meshes (Fig. S11; Table S4). The decrease in mean depth followed the decrease in resolution for the regular grid-based meshes, while the average for the CS mesh is very similar to the R100 mesh. While the differences of the median are relatively small, the spread of these values

Table 2
Summary of goodness-of-fit between modeled and measured values, for the calibration and validation of mesh and hydraulic modeling results. Table parameters: discharge Q: type (calibration C or validation V); variable; number of observations (# obs.); mesh type; bias, avg. ± stand. deviation (minimum/ maximum values); RMSE; slope and intercept, avg. ± stand. error, for measured vs. modeled linear fit (with * indicating p-value < 0.05 m and ** < 0.001),; coefficient of determination R^2; Nash–Sutcliffe efficiency (NSE).

Q (m^3/s)	type	variable (unit)	# obs.	mesh	bias (m)	RMSE (m)	slope	intercept	R^2	NSE
1.7	C	WSE (cm)	116456	R25	0.00 ± 0.08 (-0.71/ 1.07)	0.08	1.00 ± 0.00**	2.94 ± 0.06	1.00	1.00
			29187	R50	0.01 ± 0.08 (-0.41/ 1.04)	0.08	1.00 ± 0.00**	2.25 ± 0.12	1.00	1.00
			7824	R100	0.01 ± 0.08 (-0.64/ 0.96)	0.08	1.00 ± 0.00**	0.72 ± 0.24	1.00	1.00
			4705	CS	−0.01 ± 0.12 (-0.85/ 0.85)	0.12	1.00 ± 0.00**	−4.13 ± 0.46	1.00	1.00
	V	flow velocity (cm/s)	30	R25	0.00 ± 0.14 (-0.33/ 0.34)	0.13	1.16 ± 0.10**	−0.07 ± 0.05	0.84	0.83
				R50	−0.02 ± 0.16 (-0.35/ 0.34)	0.16	1.23 ± 0.12**	−0.12 ± 0.06	0.79	0.76
				R100	−0.00 ± 0.17 (-0.36/ 0.35)	0.16	1.21 ± 0.13**	−0.12 ± 0.07	0.76	0.74
				CS	−0.07 ± 0.27 (-0.59/ 0.34)	0.27	0.74 ± 0.18**	0.07 ± 0.10	0.37	0.28
10.4	V	water's edge - vertical Z (cm)	104	R25	−0.01 ± 0.12 (-0.21/ 0.55)	0.12	0.99 ± 0.00**	6.83 ± 3.86	1.00	1.00
				R50	0.01 ± 0.12 (-0.19/ 0.60)	0.12	1.00 ± 0.00**	4.17 ± 3.89	1.00	1.00
				R100	0.03 ± 0.11 (-0.18/ 0.64)	0.12	1.00 ± 0.00**	1.22 ± 3.91	1.00	1.00
				CS	0.01 ± 0.16 (-0.44/ 0.56)	0.16	0.99 ± 0.01**	9.71 ± 5.28	1.00	1.00
		water's edge - planar XY (m)		R25	0.22 ± 1.12 (-3.41/ 5.68)	1.14				
				R50	0.31 ± 1.51 (-9.88/ 5.58)	1.53				
				R100	0.47 ± 1.56 (-9.93/ 5.49)	1.63				
				CS	0.22 ± 1.12 (-3.41/ 11.46)	3.04				

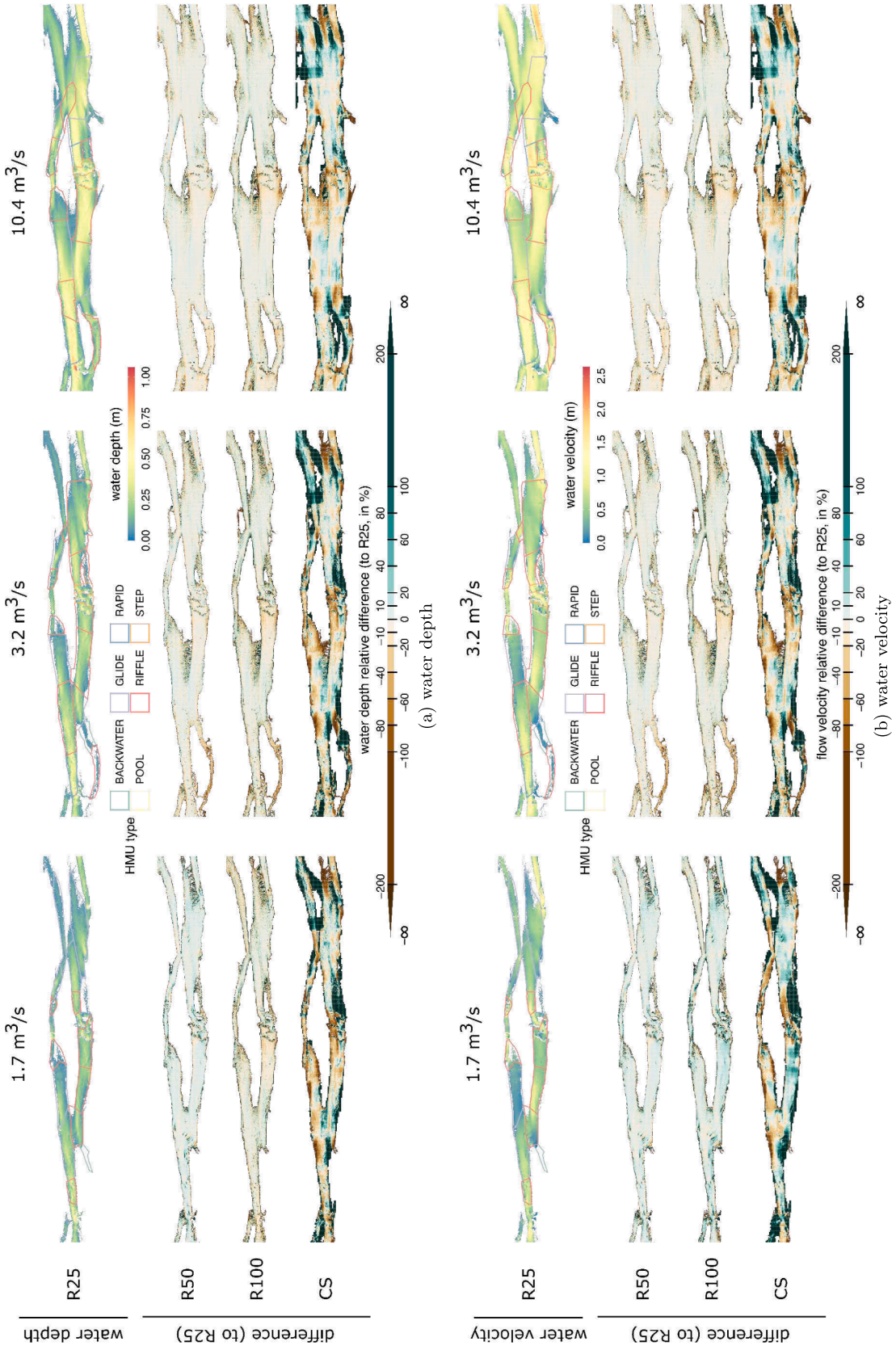

Fig. 6. Spatial variability of modeled water depth (a) and velocity (b). Depth and velocities are shown for the R25 mesh (used as reference; upper row in each panel), on which the mapped mosaic of surveyed HMUs is overlaid. The three rows below show spatially explicit relative difference maps ($(x_{comp} - x_{ref})/x_{ref} \cdot 100\%$, with $x_{ref/comp}$ expressing modeled water depth and flow velocity obtained in the reference mesh) between simulated depths (a) and velocities (b) using the meshes R50, R100 and CS and the reference R25. A comparison is given for the meshes R50, R100 and CS. Computational cells with simulated depth below a threshold of 0.05 m are considered as dry.

Table 3
Comparison of HMU-based statistics (mean and SD) to reference (R25) for depth and velocity distributions corresponding to R50, R100, CS and field survey. The quality of agreement between the different geometric configurations and approaches is expressed in terms of slope and intercept of the linear fit of reference to comparison values (avg. ± std. error), the coefficient of determination (R^2) and Root Mean Squared Error (RMSE).

	depth							
	mean				SD			
	slope	intercept	R^2	RMSE (m)	slope	intercept	R^2	RMSE (m)
R50	1.01 ± 0.01	0.00 ± 0.00	1.00	0.01	1.00 ± 0.01	0.00 ± 0.00	1.00	0.00
R100	1.03 ± 0.01	1.00 ± 0.00	0.99	0.01	0.99 ± 0.01	0.01 ± 0.00	0.99	0.01
CS	1.02 ± 0.01	0.01 ± 0.01	0.92	0.04	1.01 ± 0.06	0.01 ± 0.01	0.85	0.03
survey	0.66 ± 0.08	0.04 ± 0.03	0.58	0.12	0.18 ± 0.11	0.10 ± 0.01	0.05	0.07
	velocity							
	mean				SD			
	slope	intercept	R^2	RMSE (m/s)	slope	intercept	R_2	RMSE (m/s)
R50	0.94 ± 0.01	0.02 ± 0.01	0.99	0.03	0.97 ± 0.02	0.01 ± 0.00	0.98	0.01
R100	0.93 ± 0.02	0.01 ± 0.01	0.98	0.05	1.02 ± 0.03	0.01 ± 0.01	0.96	0.02
CS	0.77 ± 0.07	0.11 ± 0.05	0.73	0.16	0.90 ± 0.09	0.04 ± 0.02	0.65	0.06
survey	0.69 ± 0.05	0.11 ± 0.04	0.79	0.19	0.56 ± 0.07	0.07 ± 0.02	0.56	0.09

increased for coarser mesh types, with an SD of respectively 3.0, 4.2 and 19.9 % for the R50, R100 and CS meshes. A similar pattern can be observed for residual differences in the SD of the distributions, with median differences increasing up to 12.9 % for the CS results, and a spread of the residuals increasing from 6.1 % for R50 to 25.8 % for CS. For the velocities, similar patterns as for the depth were observed. The mean velocity increased with decreasing mesh resolution and quality. Particularly affected were the results of CS, which although having a relatively small median, have a spread of 298.9 %. Similarly, the mean SD residual of the velocity distributions decreased consistently with a decrease in mesh resolution for R50 and R100. While the average CS residual SD is similar to R100, the spread of the residuals was also higher. The highest disagreement was found when comparing surveyed frequency distributions, both for the mean and SD of residuals. Compared to reference, measurements tended to overestimate the HMU-averaged depth and velocity by about 28.1 and 24.6 % respectively, and also differed consistently in terms of SD, which showed a median average residual of −7.4 and 20.4 %. The spread of these values was also the highest amongst the approaches, with the only exception observed for the mean velocities of the CS results. All values from this analysis are reported in Table S4 in the supplementary materials. Finally, it must be noted that, with exception of the SD residuals for the depth of survey, and the mean residuals of velocity for CS, all approaches differed significantly from reference (Table S4).

A comparison of residual differences in mean and SD by mesh type and HMU type is shown in Fig. 7. The patterns described above for the reach level analysis, remained fairly consistent also on an HMU type basis, with a larger spread of the values for the lesser resolution and quality meshes, as it can be easily seen by the larger confidence intervals (Table S5). The largest differences were observed for backwaters, with substantial differences also amongst approaches. Morphologically complex units such as pools, rapids and steps showed also a higher sensitivity towards the choice of descriptive approach, while morphologically less complex units, such as glides and riffles, were less sensitive. However, the mesh choice in 2D modeling can strongly affect the residual SD of the distributions. No consistently positive or negative effect on the residuals of mean and SD for the choice of approach at the HMU level was identified, as shown by the results of the Wilcoxon test (Table S5).

A comparison of sensitivity ranges between the approaches (Table 4) highlighted the most sensitive HMU types to the choice of hydraulic description. Amongst the 2D modeling results, backwaters had the

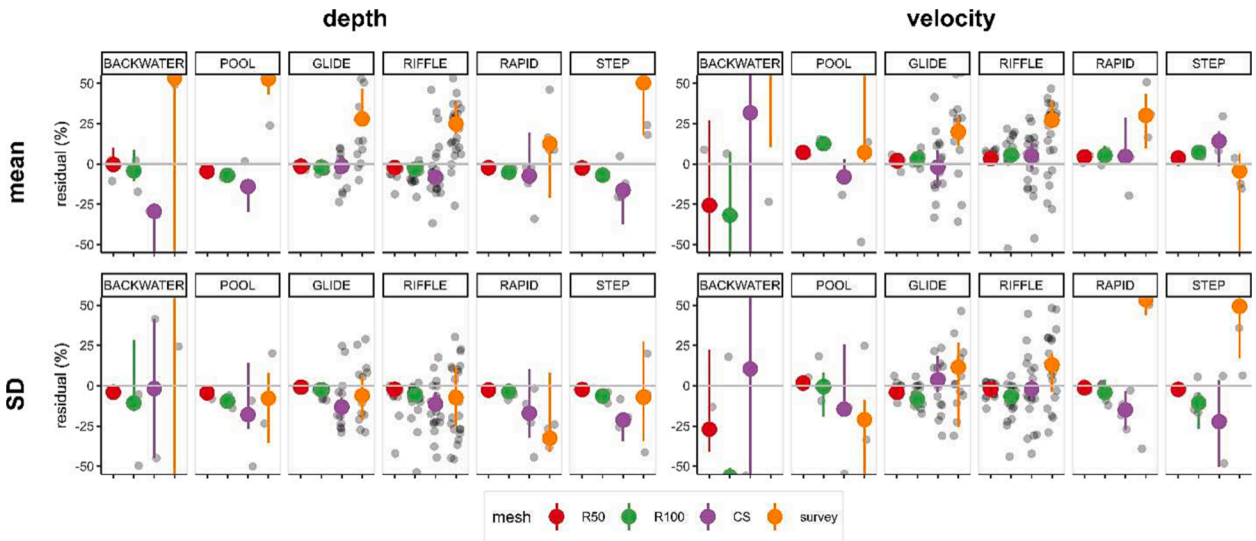

Fig. 7. Comparison of mean and SD of residual differences between approaches (R50, R100, CS and survey) and their reference (R25) for water depth and velocity, grouped by HMU types. In the graph, the large colored dots represent the median value, with the bars visualizing its 95% Confidence Interval. The smaller black dots are the actual values. To improve readability, the range of the y-axis was reduced, and some larger values were omitted from the graph. A full description of the data is presented in Table S5 in supplementary materials.

Table 4
Range comparison of hydraulics residuals by approach and HMU type. The "median range" ($|max(median(x)) - min(median(x))|$) and the "total range" ($|max(x) - min(x)|$) of the residual values x (in %) between all considered approaches are shown. The "2D modeling" table (a) shows ranges for R50, R100 and CS. The "all approaches" tables (b) also includes survey.

(a) 2D modeling

	median range (%)				total range (%)			
	depth		velocity		depth		velocity	
	mean	SD	mean	SD	mean	SD	mean	SD
backwater	29.0	9.0	63.7	67.0	121.3	91.1	2272.9	153.4
pool	9.5	13.5	20.6	16.3	15.9	46.4	34.7	73.0
glide	0.6	12.4	4.8	11.9	33.6	53.6	74.7	54.6
riffle	6.1	9.2	2.3	4.6	82.8	152.1	268.8	166.4
rapid	5.1	14.4	0.8	13.8	32.9	43.3	28.0	28.6
step	13.7	18.9	10.5	20.0	25.4	23.8	26.7	54.2

(b) all approaches

	median range (%)				total range (%)			
	depth		velocity		depth		velocity	
	mean	SD	mean	SD	mean	SD	mean	SD
backwater	82.8	163.7	98.4	332.9	532.7	657.6	2272.9	413.8
pool	66.8	13.5	20.6	22.7	77.1	70.3	63.9	79.6
glide	29.9	12.4	22.0	19.9	189.4	331.8	92.6	155.6
riffle	33.3	9.2	23.8	19.7	157.5	219.4	268.8	166.4
rapid	20.1	29.9	25.7	68.4	80.3	72.2	70.4	102.1
step	66.7	18.9	18.6	71.6	103.5	61.4	82.5	129.9

highest ranges for all parameters, both for median and total ranges. High range values were also observed for the topographically more complex units, such as pools, steps and rapids. When comparing glides and riffles, the results show that glides are overall less sensitive, particularly when the total spread of residuals is compared, as represented by the total range.

Generally, it was also observed that water depth was overall less sensitive in terms of choice of approach compared to velocity.

3.4. Sensitivity of mesohabitat suitabilities

3.4.1. Comparison at the HMU scale

Based on suitability maps (an example of which is provided in Fig. 8; see also Fig. S12 and S13 in suppl. materials for the discharges 3.2 and 10.4 m^3/s), concordance maps for the marble trout (adult and juvenile), and the European bullhead (adult) were computed, for the three surveyed discharges based on a hydraulic description from all considered approaches (Fig. 9). It can be observed that many HMUs showed a high concordance among all approaches, with a few HMUs being particularly affected. While the adult life stages show disagreement at all discharges, full concordance is observed for the juvenile marble trout at the highest flow.

A visual summary of concordance by HMU type can be seen in Fig. 10. Table 5 reports Cohen's Kappa (k) values for inter-model agreement between approaches and the references, while a summary (of the % of full concordance) by approach, HMU type and species is reported in Table S6. When comparing the two-dimensional modeling approaches, it can be observed that concordance decreases with decreasing mesh resolution and quality, with almost full concordance for the R50 set-up (k = 0.95), and a lower degree for the CS set-up (k = 0.69). The highest differences are found between the reference and the survey (k = 0.47). When comparing the level of concordance by HMU type, the highest disagreements are found for backwaters (33.3 %, k = 0.61), pools (55.5 %, k = 0.63) and rapids (58.3 %, k = 0.71), while the highest agreement levels are for glides (72.9 %, k = 0.82) and riffles (65.3 % for all species and approaches, k = 0.73).

3.4.2. Comparison of habitat-streamflow rating curves

When comparing the resulting habitat - streamflow rating curves between all approaches and the reference (Fig. 11), it can be observed that all curves follow similar patterns, although punctual differences can be found in terms of estimated suitable channel area. A comparison in

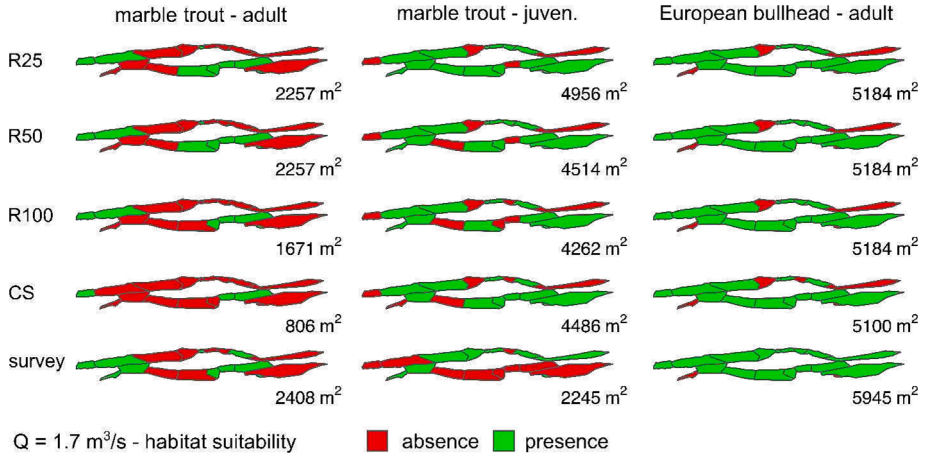

Fig. 8. Comparison of habitat suitabilities for all species and approaches, at $Q = 1.7 m^3/s$.

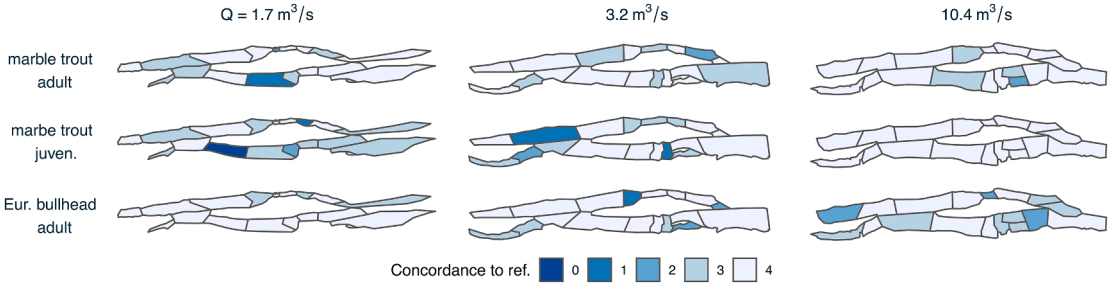

Fig. 9. Concordance maps of habitat suitability maps (by Q and species). All approaches (R50, R100, CS and survey) are compared against reference (R25). Concordance is computed as the sum of agreements between approaches and the reference.

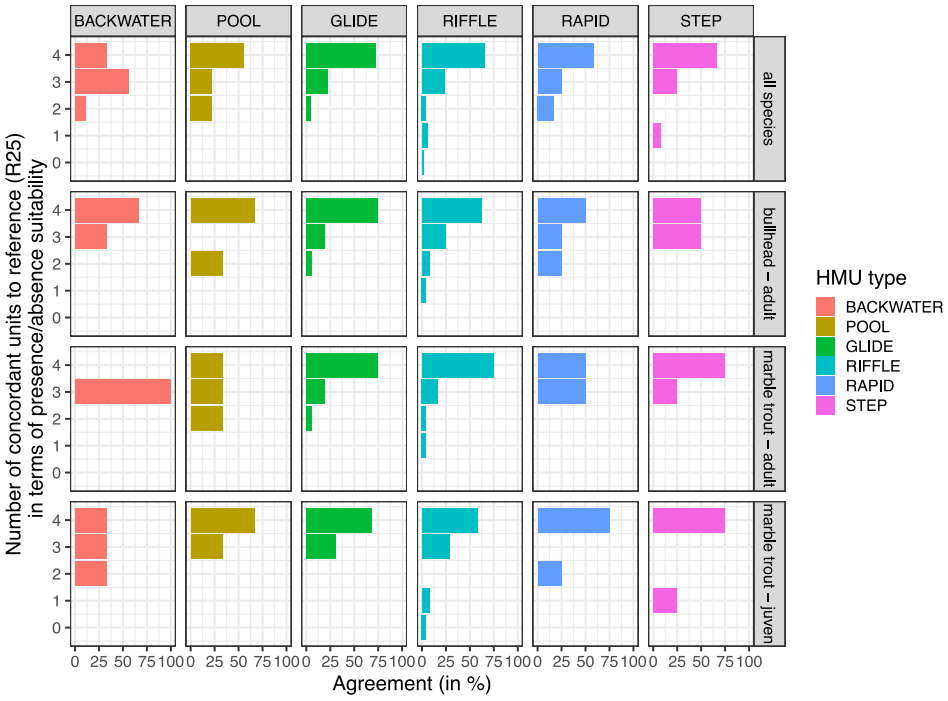

Fig. 10. Comparison of concordance of suitability against reference (R25) by HMU type, for all approaches (R50, R100, CS, survey). The results are divided by species and life-stage, and combined together (in all species). Total concordance (y-axis) is computed as the sum of agreements between approaches and the reference, and shown as a percentage (colored bars). In the legend, the total number of units per HMU type is shown.

Table 5
Inter-model agreement comparison, computed as Cohen's Kappa, with n the number of compared observations. (a) Comparison by modeled species (MA: marble trout; B: Eur. bullhead); (b) comparison by HMU type.

(a)

species:	MA adult	MA juven.	B adult	all
n		54		162
R50	1.00	0.88	0.94	0.95
R100	0.92	0.79	0.89	0.89
CS	0.66	0.68	0.62	0.69
survey	0.51	0.39	0.26	0.47

(b)

mesh:	n	R50	R100	CS	survey	avg.
backwater	9	1.00	1.00	0.18	0.25	0.61
pool	9	1.00	0.57	0.77	0.18	0.63
glide	48	1.00	1.00	0.81	0.48	0.82
riffle	72	0.89	0.86	0.69	0.47	0.73
rapid	12	1.00	0.82	0.47	0.53	0.71
step	12	1.00	0.80	0.50	0.64	0.73

terms of R^2 and nRMSE is presented in Table 6. Overall, R50 had the highest performance amongst all approaches when compared to reference ($R^2 = 0.99$ and nRMSE $= 3$ %), and survey had the lowest ($R^2 = 0.799$ and nRMSE $= 17$ %). However, results are dependent on species and life-stage. The largest differences were found for the juvenile marble trout and the adult bullhead, for which survey, although maintaining a similar pattern to reference, had the highest error (27 and 25 % respectively). Nonetheless, almost all curves obtained through the different approaches displayed a consistent shape, in terms of location and values of maxima, minima and inflection points. Differences from the curve are also reflected in area values estimated for individual discharges. For e.g. the mean-annual-low flow ($Q = 1.57 m^3/s$), the following suitable areas are estimated for the adult marble trout: 2084.5 m^2 for R25 and R50, 1543.6 m^2 for R100, 744.5 m^2 for CS and 2224.2 m^2 for survey. For $Q_{90} = 1.71 m^3/s$, i.e. the flow that is exceeded 90 percent of the time, areas for the adult bullhead range from 5116.4 (CS) to 5959 m^2 (survey).

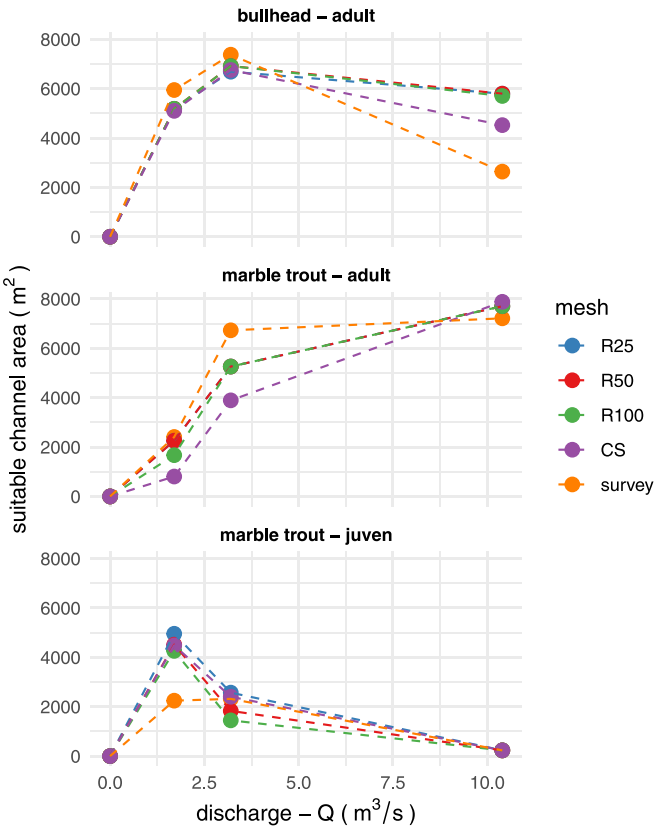

Fig. 11. Comparison of habitat - streamflow rating curves. All approaches (R50, R100, CS and survey) are compared, including reference (R25).

4. Discussion

4.1. Sensitivity of the hydraulic description

A median decrease (towards larger negative values) in residual mean depth and SD with decreasing mesh resolution and quality was observed for the 2D hydraulic modeling results. Geometric configuration and resolution also affected the spread of these values, with the most inconsistent results (i.e. having the highest spread) found for the CS mesh. A similar effect was observed for the mean and SD of velocity, which however tended to be overestimated. The median residual difference and the residual spread of velocities were higher than for depth. This is in agreement with previous works, which showed that simulated water velocities are more sensitive on the choice of mesh than water depth (Horritt et al., 2006; Williams et al., 2013). Pasternack et al. (2006) found that a computational mesh derived from low resolution topographic surveys, which were unable to accurately represent the complex topographical structures of the reach, resulted in errors up to 20% for simulated depth and velocity. In accordance, Conner and Tonina (2014) found that for micro-habitat modeling, only a cross-section spacing of 0.5 to 1 average channel widths (W) could achieve results similar to a complete high resolution grid, while a spacing higher than 2 W resulted in simplified flow structures, and higher than 4 W tended towards a pseudo-1D solution, which is unsuitable for habitat modeling. In this work a variable spacing of $\sim 0.3-2.5$ W was used, which was adjusted to the local conditions of the channel.

The lowest similarity was found for the survey-based hydraulic description, for which higher values of both average depth and flow velocity were observed, and which had the highest spread of residuals, when compared with the results of the reference hydraulic simulation (R25). In the MesoHABSIM methodology, a stratified-random approach (Parasiewicz, 2007) is used to sample water depth and flow velocities within each HMU, which requires the field operator to subjectively decide (i) where to sample depth/velocity, and (ii) how many points are needed to describe the heterogeneity of the flow in each HMU. A likely cause of the large discrepancies between modeled and surveyed hydraulic descriptions are the much lower average densities of points surveyed in this study ($0.044 pts./m^2$), which were about 11 to 340 times lower than modeled ones (15, 4, 1 and $0.5 pts./m^2$ respectively for R25, R50, R100 and CS). The lower number of sampled points likely led to an under-sampling of marginal areas, which could be better represented by hydraulic modeling. Operator subjectivity can be affected by challenging flow conditions and limited visibility, due to e.g. high turbidity or when sampling larger HMUs, which make it difficult to properly assess the range of conditions present in them. Results can also be affected by variability between operators surveying together and by a tendency to better recognize larger contrasts, which makes it easier to e.g. distinguish very fast and turbulent flows from calmer areas within a step and pool sequence, but more difficult to discern small differences in velocity within a more homogeneous glide or riffle (Roper et al., 2002; Maddock and Hill, 2004; Bangen et al., 2014). Discrepancies between modeled and surveyed velocities, could also be due to the high uncertainties associated both with in-stream surveying of velocities (Kondolf et al., 2000; Boavida et al., 2013), and their spatially distributed estimation implementing 2D hydraulic models (Pasternack et al., 2006; Williams et al., 2013; Boavida et al., 2013), as also seen within this study (RMSE of 0.13 to 0.27 m/s).

Further discrepancies between surveyed and modeled flow values, particularly when comparing water edges at high flow during hydraulic model validation (Table 2), could be explained by some minor morphological change that might have occurred between the time of LiDAR bathymetric survey and the MesoHABSIM survey at the highest flow (2016–2018), due to few small floods. While changes were negligible in the analyzed reach, more substantial erosion and deposition were observed in the wider modeled reach (Baumgartner, 2020).

Similar patterns as the reach-scale analysis were also found when comparing the results by HMU type, with an approach-dependent increase in residual differences. The most sensitive HMU was the backwater, followed by morphologically complex units such as rapids, steps and pools. The lowest residual values and sensitivity ranges were found for riffles and particularly glides. The inconsistencies of higher sensitivity of backwaters to the chosen approach could be caused by their relatively smaller sizes and water depths when compared to other HMU types (Fig. S10). Smoothing due to lower mesh resolutions or the interpolation from cross-sections decreases the quality of the hydraulic

Table 6
Comparison of habitat - streamflow rating curves for all approaches (R50, R100, CS and survey) against reference (R25). Suitability was estimated for the species marble trout (adult and juvenile), European bullhead (adult) and for all pooled species and life stages. The quality of agreement between the different geometric configurations and approaches is expressed in terms of the coefficient of determination (R^2) and nRMSE.

	marble trout (adult)		marble trout (juven.)		Eur. bullhead (adult)		all species	
	R^2	nRMSE(%)	R^2	nRMSE(%)	R^2	nRMSE (%)	R^2	nRMSE(%)
R50	1.000	0	0.985	9	0.999	2	0.992	3
R100	0.993	4	0.962	13	0.998	2	0.982	5
CS	0.942	13	0.999	5	0.955	10	0.954	9
survey	0.942	10	0.804	27	0.694	25	0.799	17

description, which more strongly affects units such as steps and rapids due to their higher morphological complexity than glides and riffles. These units are characterized by more homogeneous flow conditions and less water surface variability through space, which also facilitates their accurate survey. Such decrease in accuracy for coarser meshes agrees with Waddle (2010), who investigated the effects of mesh density on water depth and velocity estimates around and near boulders. While only minimal differences between modeled and ALB-derived water depths were observed between HMU types (Fig. S8), higher uncertainties in the modeled values, particularly for flow velocities, could be expected for steeper and more complex units such as steps and rapids. Shallow water 2D hydraulic modeling requires streambed slopes below 10 % (Miller and Cluer, 1998) and negligible vertical accelerations (Shen and Diplas, 2008) for meaningful results, which are typical of lower energy HMU types such as glides and riffles, where we also observed the lowest discrepancies between approaches.

4.2. Sensitivity of habitat suitabilities

In agreement with hydraulic findings, backwaters showed the smallest concordance of presence/absence suitability between approaches with the reference, while glides exhibited the highest agreeement, and were less sensitive than riffles also in terms of suitability. Steps, on the other hand, displayed smaller sensitivity as they were generally unsuitable for the analyzed species, particularly for the marble trout's juvenile life stage, which made them less affected by differences in hydraulic description.

Coherently, comparing habitat-streamflow rating curves to the reference R25 results, showed that R50 results had the highest R^2 values and lowest errors, while R100 and CS results showed smaller correlations and larger errors. The largest differences were found for survey-derived results, particularly for the juvenile marble trout, for which the curve poorly represented the reference curve's maxima. The motivation is that juvenile stages require low depths and velocities, while the measurements tended to overestimate water depth and velocities compared to the R25 reference. CS results had the second highest error compared to reference, as they generally underestimated water depths and velocities. Despite such differences, values and locations of maxima, minima and inflection points of the habitat-streamflow rating curves were coherent among approaches, suggesting an interesting scale-dependence in the sensitivity of habitat suitability to the different approaches used to estimate it. The sensitivity reduces when moving from the individual HMU scale (Geomorphic Units, sensu Belletti et al., 2017) to the reach scale (sensu Rinaldi et al., 2017).

Results from this analysis also suggest that the HMU composition of the reach affects the sensitivity of the estimated reach habitat suitability, which is higher when more backwaters or morphologically complex unit types are present.

Substrate or the presence of covers, known as important habitat descriptors (Parasiewicz, 2007; Vezza et al., 2014; Negro et al., 2021; Wegscheider et al., 2021), were not accounted for in the sensitivity analysis. This allowed focusing only on the effects of changes in water depth and flow velocities on estimated habitat suitabilities. Including these variables would likely affect results, as unsuitable substrate or absence of covers would persist regardless of hydraulic changes, requiring the adoption of biological models able to account for substrate and cover preferences as well.

4.3. Practical implications of the study

The study shows that 2D hydraulic modeling for meso-scale habitat modeling in medium to large low-gradient rivers (e.g. gravel-bed rivers mostly composed by glides and riffles) is very robust to the choice of mesh. In-stream surveys also yield similar results in such cases. A quick mesohabitat survey to assess the HMU composition of the reach could guide the choice of modeling approach. Higher resolution DTMs and meshes, which are able to correctly reproduce the topographical features within the reach and to represent macro-roughness elements such as large boulders, are required when a high number of morphologically complex HMUs are present in the modeled reach.

Choosing an optimal mesh quality and resolution can significantly reduce modeling effort (in terms of modeling time) while mantaining predictive performance to the required level. In this study, for example, the R50 mesh provided similar results to the R25 mesh but reduced computational effort by a factor of 7 (Table 1), making it a preferable choice in terms of predictive performance-to-modeling effort ratio.

Finally, our study suggest that the ability to represent maxima, minima and inflection points of the habitat-streamflow rating curves, is less sensitive to the approach used to describe the hydraulics with respect to the description of the hydraulics of individual HMUs within the reach. For cases where only relative habitat suitability estimates are required, during e.g. an environmental flow assessment, opting for a less accurate but less resource-intensive approach can significantly reduce time and resources effort.

4.4. Study limitations and suggested future research

Besides their intrinsic limitations, the results of this work also provide a set of suggestions for future research on the topic.

The results suggest that the different sensitivities between HMU types could be explained by their different morphological structure and complexity. The highest sensitivities were found for backwaters, rapids and pools, which were however under-represented in the reach. Future studies should consider a more balanced distribution of unit types and could look into what morphological structures (e.g. the presence of large boulders) within the same unit types more strongly affect the outcomes of hydraulic modeling.

When relating to existing work this analysis highlights the relevance of spatial scales ranging from: the individual channel width (e.g. Conner and Tonina, 2014) down to a representative macro-roughness size (e.g. boulders, Niayifar et al., 2018). To generalize sensitivity results from hydraulic modeling, a wider range of grid resolutions and cross-sectional spacing should be tested, to sistematically explore the role of these two main morphological spatial scales. The size of mesohabitats scales with the channel width (Belletti et al., 2017), and the resolution of the computational mesh should correctly represent macro-roughness elements within the channel (Baumgartner, 2020), and allow to describe relevant eco-hydraulic processes (Pasternack, 2011). In this study, while all meshes had consistently lower resolutions than the average wetted channel width, only the R25 and R50 meshes had resolutions much lower than the average macro-roughness size of the reach (Table 1).

In habitat modeling, values for water depth and flow velocity are often binned into classes with a specific width (15 cm and 15 cm/s in this study). While residual differences in mean and SD of water depth and flow velocities between the approaches were high, absolute differences tended to fall within 1–20 cm (or cm/s) on average (Table 3), corresponding to a shift of the values of 1–2 classes. Since strict tresholds for water depth and velocity were used in the categorical biological models implemented in this study, when hydraulic conditions within an HMU are close to the thresholds of the suitability models, even small differences in their values could result in a change in presence/absence prediction. Sensitivities for habitat suitability estimates might hence also depend on the choice of such thresholds, and the width of water depth and velocity bins.

To allow a full comparison between surveys and hydraulic modeling results, only three discharges were compared. Such a comparison might however mask differences in habitat-streamflow relationships, such as in peak habitat discharge. By using methodologies to model the meso-scale habitat mosaic from the outputs of 2D hydraulic models (e.g. Legleiter and Goodchild, 2005; Hauer et al., 2009; van Rooijen et al., 2021; Farò et al., 2022), future comparisons could include a wider range of flow

conditions.

Given the wide range of approaches implementing habitat modeling in the field of environmental flow assessments (Bovee, 1982; Capra et al., 1995; Maddock, 1999; Parasiewicz, 2007; Jowett and Biggs, 2010; Holzapfel et al., 2014; Vezza et al., 2015), a more comprehensive sensitivity analysis would be challenging, because of the specificity of each environmental flow assessment and habitat modeling approach. Following the workflow presented in this work, ad hoc analysis could be however performed, to study e.g. the sensivity of habitat suitability estimates to a pre-defined discharge, or to the peak-discharge derived from the habitat-streamflow curve.

Finally, the possibility of exploring differences in sampling density and surveying approaches, such as a relationship between densities of measured points and HMU types, could provide an important contribution to the methods of instream habitat surveys, by increasing the accuracy of surveying protocols.

5. Conclusions

In the present study the sensitivities of meso-scale hydraulic description and the resulting habitat suitabilities at the meso-scale on the chosen approach for the spatial description of the flow hydraulics in habitat modeling were tested. Three commonly used approaches were compared: 2D hydraulic modeling based on high resolution computational meshes derived from airborne LiDAR bathymetry surveys; 2D hydraulic modeling based on a low quality and low resolution mesh, which was reconstructed from cross-sectional profiles of the topo-bathymetry; and in-stream surveys. The 2D modeling results, based on the regular grid mesh with the highest resolution of 25 cm were used as reference.

Mean and SD of the Hydro-Morphological Units (HMU)-based distributions of water depth and velocities were affected by a decrease in mesh resolution and mesh quality, both in terms of residual difference and spread of the residuals, with the largest differences between the 2D hydraulic modeling approaches found for the cross-section based model results. Overall, the largest disagreement was found for the in-stream survey based description, which tended to overestimate both water depths and velocities in comparison with the highest resolution model results. In our study reach, backwaters were found the HMU type most sensitive to the choice of approach, followed by morphologically complex units such as pools, rapids and steps. Riffles and particularly glides showed the smallest level of sensitivity. Similar results were found when comparing presence/absence fish habitat suitabilities for two species, the marble trout and the European bullhead. However, while the differences at the HMU scale could be quite high, when comparing estimated suitable channel habitat areas at the reach scale, and with varying discharge, the differences became less evident. In particular, while the magnitude of the estimated habitat suitabilities differed, with the lowest correlation to the reference curves found for the cross-section-based and the in-stream survey derived results, the resulting habitat-streamflow rating curves were similar in terms of their shape and overall trends for all tested approaches, correctly identifying maxima, minima and inflection points.

From a water management point of view, the results presented in this work suggest that the HMU composition of the reach strongly affects the sensitivity of the estimated reach habitat suitability on the choice of approach. When the percentage of backwaters and morphologically complex HMUs such as steps, pools and rapids is high, a more accurate approach for the description of the reach hydraulics should be chosen. On the other hand, glides and riffles seem to be less sensitive to the choice of the approach, and more economical and faster approaches, such as 2D modeling based on densely spaced (spacing $<$ channel-width) cross-sectional topographical profiles could be used. However it must be noted, that the spacing of the cross-sections should be able to represent the morphological variability of the reach. A quick field appraisal of the HMU mosaic composition of the reach could therefore be used to guide the choice of descriptive approach.

CRediT authorship contribution statement

David Farò: Conceptualization, Methodology, Investigation, Writing - original draft, Writing - review & editing. **Katharina Baumgartner:** Methodology, Investigation, Writing - original draft. **Paolo Vezza:** Supervision, Writing - review & editing. **Guido Zolezzi:** Supervision, Writing - review & editing, Funding acquisition.

Declaration of Competing Interest

The authors declare that they have no known competing financial interests or personal relationships that could have appeared to influence the work reported in this paper.

Acknowledgments

Financial support was received by the Italian Ministry of Education, University and Research (MIUR) under the Departments of Excellence, grant L.232/2016 and by the Autonomous Province of Bolzano/Bozen, under the research project “FHARMOR Fish Habitat in Alpine rivers: integrating monitoring, modeling and remote sensing”, funding agreement n. 17/34 of 03/11/2016. A thanks goes also to Giovanni Negro, who provided the conditional habitat suitability models, and to the many collegaues that supported field work. The manuscript was greatly improved following suggestions from two anonymous reviewers.

Appendix A. Supplementary data

Supplementary data associated with this article can be found, in the online version, at https://doi.org/10.1016/j.hydroa.2023.100160.

References

Acreman, M.C., Dunbar, M.J., 2004. Defining environmental river flow requirements - a review. Hydrol. Earth Syst. Sci. 8 (5), 861–876.
Adamczyk, M., Parasiewicz, P., Vezza, P., Prus, P., De Cesare, G., 2019. apr). Empirical Validation of MesoHABSIM Models Developed with Different Habitat Suitability Criteria for Bullhead Cottus Gobio L. as an Indicator Species. Water 11 (4), 726.
Anderson, K., Paul, A., McCauley, E., Jackson, L., Post, J., Nisbet, R., 2006. Instream flow needs in rivers and streams: The importance of understanding ecological dynamics. Front. Ecol. Environ. 4 (6), 309–319.
Bangen, S., J. Wheaton, N. Bouwes, C. Jordan, C. Volk, M.B. Ward (2014). Crew variability in topographic surveys for monitoring wadeable streams: A case study from the Columbia River Basin. Earth Surface Processes and Landforms 39(15), 2070–2086.
Barker, J.R., Pasternack, G.B., Bratovich, P.M., Massa, D.A., Wyrick, J.R., Johnson, T.R., 2018. feb). Kayak drifter surface velocity observation for 2D hydraulic model validation. River Res. Appl. 34 (2), 124–134.
Baumgartner, K. (2020). Analyse und Evaluierung der praktischen Anwendung von topo-bathymetrischen LiDAR Daten in alpinen Gewässern. Ph. D. thesis, Leopold-Franzens-Universität Innsbruck.
Belletti, B., Rinaldi, M., Bussettini, M., Comiti, F., Gurnell, A.M., Mao, L., Nardi, L., Vezza, P., 2017. apr). Characterising physical habitats and fluvial hydromorphology: A new system for the survey and classification of river geomorphic units. Geomorphology 283, 143–157.
Benjankar, R., Tonina, D., Mckean, J., 2015. mar). One-dimensional and two-dimensional hydrodynamic modeling derived flow properties: Impacts on aquatic habitat quality predictions. Earth Surf. Proc. Land. 40 (3), 340–356.
Blocken, B., Gualtieri, C., 2012. Ten iterative steps for model development and evaluation applied to Computational Fluid Dynamics for Environmental Fluid Mechanics. Environ. Modelling Softw. 33, 1–22.
Boavida, I., Santos, J.M., Katopodis, C., Ferreira, M.T., Pinheiro, A., 2013. Uncertainty in predicting the fish-response to two-dimensional habitat modeling using field data. River Res. Appl. 29 (9), 1164–1174.
Bovee, K.D., 1982. A guide to stream habitat analysis using the instream flow incremental methodology. In: US Fish and Wildlife Service FWS/OBS.
Capra, H., Breil, P., Souchon, Y., 1995. aug). A new tool to interpret magnitude and duration of fish habitat variations. Regulated Rivers: Res. Manage. 10 (2–4), 281–289.
Carolli, M., Zolezzi, G., Pellegrini, S., Vezza, P., 2017. Applicazione sperimentale dell'indice di integrità dell'habitat fluviale nella provincia di Trento. Technical report. Università degli Studi di Trento, Relazione Tecnica.

Conner, J.T., Tonina, D., 2014. mar). Effect of cross-section interpolated bathymetry on 2D hydrodynamic model results in a large river. Earth Surf. Proc. Land. 39 (4), 463–475.
Crowder, D.W., Diplas, P., 2000. may). Using two-dimensional hydrodynamic models at scales of ecological importance. J. Hydrol. 230 (3–4), 172–191.
Dunbar, M.J., K. Alfredsen, A. Harby (2012). Hydraulic-habitat modelling for setting environmental river flow needs for salmonids. Fisheries Management and Ecology 19 (6), 500–517.
Eisner, A., C. Young, M. Schneider, and I. Kopecki (2005). MesoCASiMiR - new mapping method and comparison with other current approaches.
Farò, D., Andreoli, A., Aufleger, M., Baran, R., Baumgartner, K., Bertoldi, W., Bussettini, M., Carolli, M., Comiti, F., Demarchi, L., Jocham, S., Klar, R., Marangoni, N., Parasiewicz, P., Politti, E., Scorpio, V., Steinbacher, F., Vezza, P., Zolezzi, G., 2018. FHARMOR: Fish Habitat in Alpine Rivers - Integrating Monitoring, Modelling and Remote sensing. In: I.S. Rivers 2018–3rd international conference on Integrative sciences and sustainable development of rivers, p. 221.
Farò, D., Baumgartner, K., Vezza, P., Zolezzi, G., 2022. A novel unsupervised method for assessing mesoscale river habitat structure and suitability from 2D hydraulic models in gravel-bed rivers. Ecohydrology 15 (7), e2452.
Fehr, R., 1987. sep). Einfache Bestimmung der Korngrössenverteilung von Geschiebematerial mit Hilfe der Linienzahlanalyse. Schweizer Ingenieur und Architekt 105 (38), 1104–1109.
Fleiss, J.L., 1971. nov). Measuring nominal scale agreement among many raters. Psychol. Bull. 76 (5), 378–382.
Gonzalez, R.L., Pasternack, G.B., 2015. oct). Reenvisioning cross-sectional at-a-station hydraulic geometry as spatially explicit hydraulic topography. Geomorphology 246, 394–406.
Hardy, R.J., Bates, P.D., Anderson, M.G., 1999. The importance of spatial resolution in hydraulic models for floodplain environments. J. Hydrol. 216 (1–2), 124–136.
Hauer, C., G. Mandlburger, H. Habersack (2009). Hydraulically related hydro-morphological units: description based on a new conceptual mesohabitat evaluation model (MEM) using LiDAR data as geometric input. River Research and Applications 25(1), 29–47.
Hauer, C., Unfer, G., Tritthart, M., Formann, E., Habersack, H., 2011. Variability of mesohabitat characteristics in riffle-pool reaches: Testing an integrative evaluation concept (FGC) for MEM-application. River Res. Appl. 27 (4), 403–430.
Holzapfel, P., B. Wagner, B. Zeiringer, W. Graf, P. Leitner, H. Habersack, C. Hauer (2014). Anwendung der Habitatmodellierung zur integrativen Bewertung von Schwall und Restwasser im Bereich der Wasserkraftnutzung. Österreichische Wasser- und Abfallwirtschaft 2014 66:5 66(5), 179–189.
Horritt, M.S., P.D. Bates, M.J. Mattinson (2006). Effects of mesh resolution and topographic representation in 2D finite volume models of shallow water fluvial flow. Journal of Hydrology 329(1–2), 306–314.
Jowett, I.G. (2010). RHYHABSIM. River hydraulic and habitat simulation. Software manual.
Jowett, I.G. and B.J. Biggs (2010). Flow regime requirements and the biological effectiveness of habitat-based minimum flow assessments for six rivers. https://doi.org/10.1080/15715124.2006.9635287 4(3), 179–189.
Kondolf, G.M., Larsen, E.W., Williams, J.G., 2000. Measuring and Modeling the Hydraulic Environment for Assessing Instream Flows. North Am. J. Fish. Manag. 20 (4), 1016–1028.
Lamouroux, N., S. Mérigoux, H. Capra, S. Dolédec, I.G. Jowett, B. Statzner (2010). The generality of abundance-environment relationships in microhabitats: A comment on Lancaster and Downes (2009). River Research and Applications 26(7), 915–920.
Lancaster, J., Downes, B.J., 2010. Linking the hydraulic world of individual organisms to ecological processes: Putting ecology into ecohydraulics. River Res. Appl. 26 (4), 385–403.
Landis, J.R., Koch, G.G., 1977. The Measurement of Observer Agreement for Categorical Data. Biometrics 33 (1), 159.
Legleiter, C.J. Goodchild, M.F., 2005. Alternative representations of in-stream habitat: Classification using remote sensing, hydraulic modeling, and fuzzy logic. International Journal of Geographical Information Science 19(March 2015), 29–50.
Maddock, I., 1999. mar). The importance of physical habitat assessment for evaluating river health. Freshw. Biol. 41 (2), 373–391.
Maddock, I., Hill, G., 2004. River Habitat Mapping: A comparison of approaches on a field workshop on the River Windrush, July 2004.pdf. Technical report, Report to the Centre for Ecology and Hydrology. CEH Wallingford.
Mandlburger, G., Hauer, C., Höfle, B., Habersack, H., Pfeifer, N., 2009. Optimisation of LiDAR derived terrain models for river flow modelling. Hydrol. Earth Syst. Sci. 13 (8), 1453–1466.
Mandlburger, G., Hauer, C., Wieser, M., Pfeifer, N., Zlinszky, A., Baghdadi, N., Thenkabail, P.S., 2015. Topo-Bathymetric LiDAR for Monitoring River Morphodynamics and Instream Habitats–A Case Study at the Pielach River. Remote Sensing 2015, Vol. 7, Pages 6160–6195 7(5), 6160–6195.
Marks, K., Bates, P., 2000. Integration of high-resolution topographic data with floodplain flow models. Hydrol. Process. 14 (11–12), 2109–2122.
McKean, J., Tonina, D., Bohn, C., Wright, C.W., 2014. Effects of bathymetric lidar errors on flow properties predicted with a multi-dimensional hydraulic model. J. Geophys. Res.: Earth Surf. 119 (3), 644–664.
Miller, A.J., Cluer, B.L., 1998. Modeling considerations for simulation of flow in bedrock channels. Geophys. Monograph-Ame. Geophys. Union 107, 61–104.
Morvan, H., Knight, D., Wright, N., Tang, X., Crossley, A., 2010. The concept of roughness in fluvial hydraulics and its formulation in 1D, 2D and 3D numerical simulation models. J. Hydraulic Res. 46 (2), 191–208. https://doi.org/10.1080/00221686.2008.9521855.
Negro, G., M. Carolli, A. Andreoli, D. Farò, G. Zolezzi, S. Fenoglio, P. Lo Conte, and P. Vezza (2022, sep). Transferability Of Mesohabitat Suitability Criteria In Northern Italy. In Proceedings of the 39th IAHR World Congress (Granada, 2022), pp. 1416–1423. IAHR.
Negro, G., Fenoglio, S., Quaranta, E., Comoglio, C., Garzia, I., Vezza, P., 2021. jul). Habitat Preferences of Italian Freshwater Fish: A Systematic Review of Data Availability for Applications of the MesoHABSIM Model. Front. Environ. Sci. 305.
Nelson, J.M., Bennett, J.P., Wiele, S.M., 2003. Flow and Sediment-Transport Modeling. In: Tools in Fluvial Geomorphology. John Wiley & Sons Ltd.
Nelson, J.M., Smith, J.D., 1989. Flow in meandering channels with natural topography. In River meandering, pp. 69–102. American Geophysical Union.
Niayifar, A., Oldroyd, H.J., Lane, S.N., Perona, P., 2018. Modeling Macroroughness Contribution to Fish Habitat Suitability Curves. Water Resour. Res. 54 (11), 9306–9320.
Noack, M., Schneider, M., Wieprecht, S., 2013. The Habitat Modelling System CASiMiR: A Multivariate Fuzzy Approach and its Applications. In: Ecohydraulics: An Integrated Approach. John Wiley & Sons, Ltd.
Nujić, M., Hydrotec (2017). Benutzerhandbuch HYDRO_AS-2D, 2D-Strömungsmodell für die wasserwirtschaftliche Praxis.
Papaioannou, G., Papadaki, C., Dimitriou, E., 2019. Sensitivity of habitat hydraulic model outputs to DTM and computational mesh resolution. Ecohydrology 13(2), e2182.
Parasiewicz, P., 2007. The MesoHABSIM model revisited. River Res. Appl. 23 (8), 893–903.
Parasiewicz, P., 2007. Using Mesohabsim to develop reference habitat template and ecological management scenarios. River Res. Appl. 23 (8), 924–932.
Parasiewicz, P., Castelli, E., Rogers, J.N., Plunkett, E., 2012. Multiplex modeling of physical habitat for endangered freshwater mussels. Ecol. Model. 228, 66–75.
Parasiewicz, P., Ryan, K., Vezza, P., Comoglio, C., Ballestero, T., Rogers, J.N., 2013. Use of quantitative habitat models for establishing performance metrics in river restoration planning. Ecohydrology 6 (4), 668–678.
Pasternack, G.B., 2011. 2D modeling and ecohydraulic analysis. University of California at Davis.
Pasternack, G.B., Gilbert, A.T., Wheaton, J.M., Buckland, E.M., 2006. Error propagation for velocity and shear stress prediction using 2D models for environmental management. J. Hydrol. 328 (1–2), 227–241.
Piñeiro, G., Perelman, S., Guerschman, J.P., Paruelo, J.M., 2008. How to evaluate models: Observed vs. predicted or predicted vs. observed? Ecol. Model. 216 (3–4), 316–322.
Pironneau, O., 1989. The Finite element methods for fluids. Wiley Chichester.
Rinaldi, M., Belletti, B., Bussettini, M., Comiti, F., Golfieri, B., Lastoria, B., Marchese, E., Nardi, L., Surian, N., 2017. New tools for the hydromorphological assessment and monitoring of European streams. J. Environ. Manage. 202, 363–378.
Roper, B.B., Kershner, J.L., Archer, E., Henderson, R., Bouwes, N., 2002. An evaluation of physical stream habitat attributes used to monitor streams. Journal of the American Water Resources Association 38(6), 1637–1646.
Schwartz, J., and J.S., 2016. Use of Ecohydraulic-Based Mesohabitat Classification and Fish Species Traits for Stream Restoration Design. Water 8(11), 520.
Shen, Y., Diplas, P., 2008. Application of two- and three-dimensional computational fluid dynamics models to complex ecological stream flows. Journal of Hydrology 348 (1–2), 195–214.
Steffler, P., Blackburn, J., 2002. River2D. Two-dimensional depth averaged model of river hydrodynamics and fish habitat. Introduction ot Depth Averaged modeling and User's Manual.
Steinbacher, F., Dobler, W., Benger, W., Baran, R., Niederwieser, M., Leimer, W., 2021. Integrated Full-Waveform Analysis and Classification Approaches for Topo-Bathymetric Data Processing and Visualization in HydroVISH. PFG – J. Photogrammetry, Remote Sensing Geoinformation Sci. 89 (2), 159–175.
Tharme, R.E. (2003, sep). A global perspective on environmental flow assessment: emerging trends in the development and application of environmental flow methodologies for rivers. River Research and Applications 19(5–6), 397–441.
Tonina, D., Jorde, K., 2013. Hydraulic modeling approaches for ecohydraulic studies: 3D, 2D, 1D and non-numerical models. In Ecohydraulics: An integrated approach (1 ed.)., pp. 31–66. John Wiley & Sons Ltd.
Tonina, D., McKean, J.A., Benjankar, R.M., Wright, C.W., Goode, J.R., Chen, Q., Reeder, W.J., Carmichael, R.A., Edmondson, M.R., 2019. Mapping river bathymetries: Evaluating topobathymetric LiDAR survey. Earth Surf. Proc. Land. 44 (2), 507–520.
van Rooijen, E., Vanzo, D., Vetsch, D.F., Boes, R.M., Siviglia, A., 2021. Enhancing an unsupervised clustering algorithm with a spatial contiguity constraint for river habitat analysis. Ecohydrology 14 (4), e2285.
Vezza, P., A. Goltara, M. Spairani, G. Zolezzi, A. Siviglia, M. Carolli, M. Cristina Bruno, B. Boz, D. Stellin, C. Comoglio, and P. Parasiewicz (2015, jan). Habitat indices for rivers: Quantifying the impact of hydro-morphological alterations on the fish community. In Engineering Geology for Society and Territory - Volume 3: River Basins, Reservoir Sedimentation and Water Resources, pp. 357–360. Springer International Publishing.
Vezza, P., Parasiewicz, P., Spairani, M., Comoglio, C., 2014. Habitat modeling in high-gradient streams: The mesoscale approach and application. Ecol. Appl. 24 (4), 844–861.
Vezza, P., Zanin, A., Parasiewicz, P., 2017. Manuale tecnico-operativo per la modellazione e la valutazione dell'integrità dell'habitat fluviale. Technical report. ISPRA.
Vreugdenhil, C.B., 1994. Numerical methods for shallow-water flow. Springer Science and Business Media.

Waddle, T., 2010. Field evaluation of a two-dimensional hydrodynamic model near boulders for habitat calculation. River Res. Appl. 26 (6), 730–741.
Wegscheider, B., Linnansaari, T., Ndong, M., Haralampides, K., St-Hilaire, A., Schneider, M., Curry, R.A., 2021. Fish habitat modelling in large rivers: combining expert opinion and hydrodynamic modelling to inform river management. doi: 10.1080/24705357.2021.1938251, 1–19.
Williams, R.D., J. Brasington, M. Hicks, R. Measures, C.D. Rennie, and D. Vericat (2013, sep). Hydraulic validation of two-dimensional simulations of braided river flow with spatially continuous aDcp data. Water Resources Research 49(9), 5183–5205.
Wright, K.A., Goodman, D.H., Som, N.A., Alvarez, J., Martin, A., Hardy, T.B., 2017. Improving Hydrodynamic Modelling: an Analytical Framework for Assessment of Two-Dimensional Hydrodynamic Models. River Res. Appl. 33 (1), 170–181.
Zerbe, S., Scorpio, V., Comiti, F., Rohrmoser, O., 2019. Vegetationsentwicklung nach einer Flussrenaturierung in den Alpen. WASSERWIRTSCHAFT 11, 18–23.